

Oil & Natural Gas Technology

Temporal Characterization of Hydrates System Dynamics beneath Seafloor Mounds: Integrating Time-Lapse Electrical Resistivity Methods and In Situ Observations of Multiple Oceanographic Parameters

Final Technical Report

Project Period: October 1, 2012 – January 31, 2015

Submitted by:

Carol Blanton Lutken, Leonardo Macelloni, Marco D'Emidio, John Dunbar, Paul Higley
August, 2015

DOE Award No.: DE- FE0010141

The University of Mississippi
Mississippi Mineral Resources Institute and
Center for Marine Resources and Environmental Technology
111 Brevard Hall
University, Mississippi, 38677
e-mail: cbl@olemiss.edu

Prepared for:

The Department of Energy - Methane Hydrates Program
United States Department of Energy
National Energy Technology Laboratory



Carol B. Lutken



Office of Fossil Energy

***Temporal Characterization of Hydrates System Dynamics beneath
Seafloor Mounds: Integrating Time-Lapse Electrical Resistivity
Methods and In Situ Observations of Multiple Oceanographic
Parameters***

Final Technical Report

Project Period: October 1, 2012 – January 31, 2015

Submitted by:

Carol Blanton Lutken, Leonardo Macelloni, Marco D'Emidio, John Dunbar, Paul Higley
CENTER FOR MARINE RESOURCES AND ENVIRONMENTAL TECHNOLOGY

111 Brevard Hall, UNIVERSITY, MS 38677

(CONTACT: CAROL LUTKEN, cbl@olemiss.edu)

Subcontractors:

John Dunbar
Department of Geology
Baylor University
PO Box 97354
Waco, Texas 76798-7354

Paul Higley
Specialty Devices, Inc.
2905 Capital Street
Wylie, TX 75098

August, 2015

DOE Award No.: DE- FE0010141

DISCLAIMER:

“This report was prepared as an account of work sponsored by an agency of the United States Government. Neither the United States Government nor any agency thereof, nor any of their employees, makes any warranty, express or implied, or assumes any legal liability or responsibility for the accuracy, completeness, or usefulness of any information, apparatus, product, or process disclosed, or represents that its use would not infringe privately owned rights. Reference herein to any specific commercial product, process, or service by trade name, trademark, manufacturer, or otherwise does not necessarily constitute or imply its endorsement, recommendation, or favoring by the United States Government or any agency thereof. The views and opinions of authors expressed herein do not necessarily state or reflect those of the United States Government or any agency thereof.”

Temporal Characterization of Hydrates System Dynamics Beneath Seafloor Mounds Integrating Time-Lapse Electrical Resistivity Methods And *In Situ* Observations Of Multiple Oceanographic Parameters

ABSTRACT

This study was designed to investigate temporal variations in hydrate system dynamics by measuring changes in volumes of hydrate beneath hydrate-bearing mounds on the continental slope of the northern Gulf of Mexico, the landward extreme of hydrate occurrence in this region. Direct Current Resistivity (DCR) measurements were made contemporaneously with measurements of oceanographic parameters at Woolsey Mound, a carbonate-hydrate complex on the mid-continental slope, where formation and dissociation of hydrates are most vulnerable to variations in oceanographic parameters affected by climate change, and where changes in hydrate stability can readily translate to loss of seafloor stability, impacts to benthic ecosystems, and venting of greenhouse gases to the water-column, and eventually, the atmosphere.

We focused our study on hydrate within seafloor mounds because the structurally-focused methane flux at these sites likely causes hydrate formation and dissociation processes to occur at higher rates than at sites where the methane flux is less concentrated and we wanted to maximize our chances of witnessing association/dissociation of hydrates. We selected a particularly well-studied hydrate-bearing seafloor mound near the landward extent of the hydrate stability zone, Woolsey Mound (MC118). This mid-slope site has been studied extensively and the project was able to leverage considerable resources from the team's research experience at MC118. The site exhibits seafloor features associated with gas expulsion, hydrates have been documented at the seafloor, and changes in the outcropping hydrates have been documented, photographically, to have occurred over a period of months.

We conducted observatory-based, *in situ* measurements to 1) characterize, geophysically, the sub-bottom distribution of hydrate and its temporal variability, and 2) contemporaneously record relevant environmental parameters (temperature, pressure, salinity, turbidity, bottom currents) to detect short-term changes within the hydrates system, identify relationships/impacts of local oceanographic parameters on the hydrates system, and improve our understanding of how seafloor instability is affected by hydrates-driven changes.

A 2009 DCR survey of MC118 demonstrated that we could image resistivity anomalies to a depth of 75m below the seafloor in water depths of 1km. We reconfigured this system to operate autonomously on the seafloor in a pre-programmed mode, for periods of months. We designed and built a novel seafloor lander and deployment capability that would allow us to investigate the seafloor at potential deployment sites and deploy instruments only when conditions met our criteria. This lander held the DCR system, controlling computers, and battery power supply, as well as instruments to record oceanographic parameters.

During the first of two cruises to the study site, we conducted resistivity surveying, selected a monitoring site, and deployed the instrumented lander and DCR, centered on what appeared to be the most active locations within the site, programmed to collect a DCR profile, weekly. After a 4.5-month residence on the seafloor, the team recovered all equipment. Unfortunately, several equipment failures occurred prior to recovery of the instrument packages. Prior to the failures, however, two resistivity profiles were collected together with oceanographic data. Results show, unequivocally, that significant changes can occur in both hydrate volume and distribution during time periods as brief as one week. Occurrences appear to be controlled by both deep and near-surface structure. Results have been integrated with seismic data from the area and show correspondence in space of hydrate and structures, including faults and gas chimneys.

TABLE OF CONTENTS	PAGE
TITLE PAGE.....	1
DISCLAIMER.....	3
ABSTRACT.....	4
TABLE OF CONTENTS.....	5
EXECUTIVE SUMMARY.....	6
INTRODUCTION.....	8
BACKGROUND.....	10
Study Site.....	11
Previous Work.....	15
EQUIPMENT.....	20
The DCR.....	20
Navigation.....	21
The SSD.....	22
The I-Spider.....	22
The IPSO Lander.....	23
Data Acquisition, Communication and Control (atom) Computer and IDP	24
METHODS.....	24
Cruise Activities.....	24
April, 2014.....	26
August-September, 2014.....	29
Post-Cruise Assessments.....	32
Battery System.....	32
Resisitivity.....	33
Oceanographic Parameters.....	33
Control Computer and IDP.....	34
RESULTS.....	35
DISCUSSION.....	38
Suggested System Modifications.....	40
CONCLUSIONS.....	41
Accomplishments.....	42
GRAPHICAL MATERIALS.....	44
REFERENCES.....	46
ACRONYMS AND ABBREVIATIONS.....	48
APPENDIX A.....	49

EXECUTIVE SUMMARY

The goal of this research was to investigate temporal variations in hydrate system dynamics by measuring changes in volumes of hydrate beneath hydrate-bearing mounds on the continental slope of the northern Gulf of Mexico, the landward extreme of hydrate occurrence in this region. Direct Current Resistivity (DCR) measurements were made contemporaneously with measurements of oceanographic parameters at Woolsey Mound, a carbonate-hydrate complex on the mid-continental slope, where formation and dissociation of hydrates are most vulnerable to variations in oceanographic parameters affected by climate change, and where changes in hydrate stability can readily translate to loss of seafloor stability, impacts to benthic communities, and venting of greenhouse gases to the water-column, and eventually, the atmosphere.

In the Gulf of Mexico, hydrate-bearing mounds occur in water depths greater than ~400m, in association with methane seeps, cold-seeps, pockmarks, and gas chimneys, and mud volcanoes, all of which appear to form, in part, in response to the vertical migration of hydrocarbon gases (mainly methane). Migration pathways for the hydrocarbon gases are commonly focused along deep-seated structural features, such as faults and fracture systems and vertical migration processes seem to accompany deformation of the host sediment. Close proximity of hydrate to the seafloor makes its stability particularly sensitive to changing seafloor conditions so increases in bottom temperatures or decreases in water-column pressure presumably shift the hydrate stability zone seaward, resulting in dissociation of shallow hydrate, release of methane, and subsequent loss of sediment strength, potentially leading to widespread collapse of the continental slope.

In order to assess the risks posed by the loss of seafloor stability and introduction of additional methane to the atmosphere and for hazards and climate modelers to quantify these risks, it is necessary to know how much hydrate exists in this setting and what conditions promote the release of methane. We focused our study on hydrate within seafloor mounds because the structurally-focused methane flux at these sites likely causes hydrate formation and dissociation processes to occur at higher rates than at sites where the methane flux is less concentrated and we wanted to maximize our chances of witnessing association/dissociation of hydrates.

Essentially all that is known about hydrate-bearing seafloor mounds has been learned from seismic data, shallow cores, and visual observations of the seafloor. Little effort had been invested in the study of *in situ* conditions of hydrates formation and dissociation and overall temporal variability of the Hydrate Stability Zone/hydrates system. Consequently, it is not possible to estimate the role of hydrates in climate change and seafloor stability without understanding the processes by which they form and dissociate.

We selected a particularly well-studied hydrate-bearing seafloor mound near the landward extent of the hydrate stability zone, Woolsey Mound (MC118). This midslope site has been studied extensively and the project was able to leverage considerable resources – including a 2009 DCR survey, 2005 multibeam, already processed and interpreted high resolution and industry seismic data, lander equipment and at-sea experience - from the team's research experience at Woolsey Mound. The site exhibits seafloor features associated with gas expulsion, hydrates have been documented at the seafloor, and changes in the outcropping hydrates have been documented, photographically, to have occurred over a period of months. In 2009, the team had conducted a survey of MC118 using the DCR method. Results identified shallow anomalies beneath the mound that have since been confirmed to contain hydrates in concentrations predicted, qualitatively, by the resistivity measurements, and related to the subsurface structures identified in seismic data.

The research included conducting observatory-based *in situ* measurements to 1) characterize, geophysically, the sub-bottom distribution of hydrate and its temporal variability, and 2) contemporaneously record relevant environmental parameters (temperature, pressure, salinity, turbidity, bottom currents) to detect short-term changes within the hydrates system, identify relationships/impacts of local oceanographic parameters on the hydrates system, and improve our understanding of how seafloor instability is affected by hydrates-driven changes.

To determine the volume and rate of change of hydrates in this dynamic environment, we modified a Direct Current Resistivity instrument and cable to conduct both survey and monitoring DCR studies while using the instrumented lander to collect relevant oceanographic data. The 2009 DCR survey of MC118 demonstrated that we could image resistivity anomalies to a depth of 75m below the seafloor in water depths of 1km. We reconfigured this system to operate autonomously on the seafloor in a pre-programmed mode, for periods of six months. We designed and built a novel seafloor lander and deployment capability that would allow us to investigate the seafloor at potential deployment sites and deploy instruments only when conditions met our criteria. This lander platform held the DCR system, controlling computers, and battery power supply, as well as instruments to record oceanographic parameters.

During the first of two cruises to the study site, we conducted resistivity surveying, selected a monitoring site, and deployed the lander and DCR array. The integrated portable seafloor observatory, or IPSO, was deployed so that the array was centered on what appeared to be the most active locations within the site, based on all available data. The equipment remained on the seafloor for 4.5 months at which time the team recovered it during a second cruise. The DCR instrument was programmed to wakeup periodically, collect a resistivity profile across the target with the array stationary on the seafloor, and then go back to sleep. This process was to have been repeated, weekly. Unfortunately, several equipment failures occurred prior to recovery of the lander and instrument packages. However, two resistivity profiles were collected together with oceanographic data. These results show, unequivocally, that significant changes can occur in both hydrate volume and distribution during time periods as brief as one week. Hydrate occurrences do appear to be controlled by structure, both deep and near-surface. Results have been integrated with existing seismic data from the same area and show correspondence in space of hydrate and structures including faults and gas chimneys.

The use of a non-standard geophysical method such as the DCR in marine hydrates assessment, the design and development of an integrated portable seafloor observatory to house and transport both the DCR array and the oceanographic sensors, and the scientific approach to investigate, temporally, *in situ* conditions of gas hydrates both geophysically and environmentally, offer immense potential to advance beyond the current understanding of gas hydrate system dynamics. Combining the investigation of shallow hydrate occurrence, volume and flux via an innovative portable lander approach promises vast new technology developments. The concept and the scientific approach the project promotes can be easily adapted to other hydrates sites worldwide as well as other extreme marine environments (hot vents, black smokers, etc.).

INTRODUCTION

Marine gas hydrates, gas molecules encased in an ice-like matrix, and stable only under extreme conditions of pressure and temperature, have been observed directly via visual surveys of the seafloor. Manned submersibles as well as Remotely Operated Vehicles (ROVs) and Autonomous Underwater Vehicles (AUVs) have recovered images of gas hydrates as well as samples, from sites throughout the world and, particularly, from the hydrocarbon-rich Gulf of Mexico (GOM). Much of what is known about marine gas hydrates has been learned from these images, seismic data, and shallow cores. Acknowledging the potential that these transient hydrocarbon-hosting compounds have as an energy resource as well as their obvious role in the stability of the seafloor hosting them and the water-column and atmosphere that receive input of gases when they dissociate, the Department of Energy (DOE), in *Charting the Future of Methane Hydrate Research in the United States* (2004), states “Understanding the temporal evolution of gas hydrate systems will require installation of long-term observatories on and beneath the seafloor.”

This charge has been largely acknowledged by the scientific community; *in situ* seafloor observatories are clearly required to enable direct measurements of geological processes affecting the formation and dissociation of gas hydrates. This approach promises to revolutionize how Earth science is done (Torres et al., 2007). Gas hydrates are prime targets for seafloor observatories because they are not static deposits, but continually change at rates that allow their evolution to be tracked on time scales that might range from less than a second to a decade or more. It is one of the few geological processes occurring at a human time scale. Climatic, oceanographic and tectonic processes affect gas hydrate stability conditions, so may produce seafloor and sub-seafloor environments that change rapidly. Observatories focused on gas hydrate-bearing sites can provide data critical for: 1) determining the factors influencing subsurface fluid flow and how this flow relates to stabilization/destabilization of gas hydrates; 2) studying the effects of microbial activity on gas hydrate processes; 3) gaining a better understanding of the role of hydrates in the global carbon cycle and their potential as an energy resource; and 4) exploring the effects of gas hydrate formation/dissociation on slope stability.

To date, little effort has been invested in the study of *in situ* conditions of formation and dissociation of hydrates or of the overall temporal variability of the hydrates system. Noteworthy exceptions include repeat visits to sites where surficial hydrates, outcropping on the seafloor have been monitored (MacDonald, et al., 2005; Juniper, 2013). Sub-bottom temporal changes in hydrate have been modeled, but not observed directly or indirectly (Liu and Flemings, 2009; Xu and Lowell, 2001). Although there is a consensus that hydrates are important in climate change and seafloor stability, particularly in environments in which conditions of temperature and pressure fluctuate in and out of the hydrate stability zone (HSZ), it is impossible to assess the magnitude of the role of hydrates without understanding the processes by which they form and dissociate.

Seafloor mounds represent one of the most diverse and least well understood settings in which hydrates are found (Aharon, et al., 1992; Roberts and Aharon, 1994). Within seafloor mounds, hydrate occurs as veins, nodules, and angular clasts encased in deformed, fine-grained sediment. It has also been found as massive outcroppings on the seafloor and as slabs of hydrate exposed above the seafloor. Hydrate-bearing mounds occur in water depths greater than 330m, worldwide, in association with a variety of other seafloor features including methane seeps (Crutchley et al., 2010), cold-seeps (Barnes et al., 2010), pockmarks (Chand et al., 2008), and gas chimneys (Netzeband et al., 2010). All of these features seem to form, in part, in response to the vertical migration of hydrocarbon gases (mainly methane), in varying degrees, as free gas, in solution, or as hydrate (Loncke et al., 2004). Migration pathways for the

hydrocarbon gases are commonly focused along deep-seated structural features, such as faults and fracture systems (Milkov and Sassen, 2001; Simonetti, et al., 2011), and vertical migration processes seem to accompany deformation of the host sediment.

Close proximity of hydrate to the seafloor makes its stability particularly sensitive to changing seafloor conditions (Reagan and Moridis, 2007); increases in bottom temperatures or decreases in water-column pressure should shift the hydrate stability zone (HSZ) seaward, resulting in dissociation of shallow hydrate and release of methane, causing over-pressures within the host sediment, and subsequent loss of sediment strength, potentially leading to wide-spread collapse of the continental slope. Evidence for events following this scenario has been found in ancient examples of uplifted margins (e.g. Kennett and Fackler-Adams, 2000). Hence, shallow hydrate in deformed mud is a more likely candidate for rapid dissociation, leading to the release of large volumes of methane into the atmosphere than other classes of marine hydrate (Dickens et al., 1997). This is particularly true for deposits near the landward edge of the current HSZ.

In order to assess the risks posed by the loss of seafloor stability and introduction of additional methane to the atmosphere and for hazards and climate modelers to quantify these risks, it is necessary to know how much hydrate exists in this setting and under what conditions the deposits release methane (Kvenvolden, 2002). Milkov (2000) estimated that there are up to 10^5 deepwater seafloor mounds worldwide, that likely 10% of these contain hydrate, and that these hydrate-bearing mounds would yield on the order of 10^8 m³ of methane each, at standard temperatures and pressures (STP). This puts the upper limit for the global amount of methane contained in mounds at 10^{12} m³ STP. For comparison, this would convert to approximately 2×10^{12} kg of CO₂, which would be about 0.1% of the total atmospheric CO₂ at 400ppm concentration. However, using slightly different methods, Milkov and Sassen (2001) estimated the total within the northern GOM alone to be on the order of 10^{13} m³ STP of methane. More recently, potentially widespread deposits of vein-fill hydrate within shallow, deformed muds have been found, not associated with mounds (Johnson, 2011). Clearly, no consensus has been reached on this topic; however, enough is currently known to justify the assumption that there is sufficient hydrate within deformed marine muds, to pose significant risk to both seafloor stability and future climate.

Using available industry data, the U.S. Bureau of Ocean Energy Management (BOEM) has identified thousands of seismic water-bottom anomalies that represent potential hydrate-bearing mounds in the northern GOM (<http://www.boem.gov/Oil-and-Gas-Energy-Program/Mapping-and-Data/Map-Gallery/Seismic-Water-Bottom-Anomalies-Map-Gallery.aspx>). We elected to focus this study on hydrate within seafloor mounds because the structurally-focused methane flux at these sites likely causes hydrate formation and dissociation processes to occur at higher rates than at sites where the methane flux is less concentrated. Furthermore, because the hydrocarbon flux at hydrate-bearing mound sites is structurally focused, these mounds may represent the exceptional case in which methane (and other hydrocarbon gases) occurs in three phases: solid hydrate, free gas, and dissolved in pore fluids (Liu and Fleming, 2007). This three-phase equilibrium is very sensitive to even small environmental changes and should also cause hydrate formation and dissociation to occur at higher rates than at sites where the methane flux is less concentrated (Liu and Fleming, 2007). Hence, hydrate-bearing mounds represent the best chance of observing hydrate system dynamics in action.

BACKGROUND

This project was designed to document temporal variations in hydrate system dynamics beneath seafloor mounds at the landward extreme of the hydrate stability field in the northern GOM. The project study area, on the continental slope, was selected to access an area where formation and dissociation of hydrate are most vulnerable to variations in oceanographic parameters affected by climate change, and where changes in hydrate stability can translate to loss of seafloor stability, impacts to benthic communities, and venting of greenhouse gases to the water-column, and eventually, the atmosphere. The objective of this project is to investigate hydrates system dynamics beneath seafloor mounds, and to conduct observatory-based *in situ* measurements to 1) characterize, geophysically, the sub-bottom distribution of hydrate and its temporal variability and 2) contemporaneously record relevant environmental parameters (temperature, pressure, salinity, turbidity, bottom currents) to investigate possible links between variability in any/all of these parameters and climate.

A photographic monitoring study conducted by MacDonald et al. (2003) demonstrated that hydrate mounds are dynamic settings in which significant change can occur over a period of a few months. Determining what is happening at depth beneath the mounds that causes these changes requires geophysical monitoring of the sub-bottom over similar periods. Seismic methods, in general, have been shown to be ineffective (Reidel et al., 2010).

Innovative Direct Current Resistivity (DCR) methods have been used successfully onshore to identify substances of anomalously high or low resistance to passing electrical current (Sheets, 2002; Wagner, et al., 2013). Hydrates, gas molecules encased in ice, are more resistive than gas, yet less so than host sediments. By combining DCR methods with standard marine methods and investigating a well-known site within the zone of hydrate stability, we hoped to create a means by which to detect these substances in the shallow subseafloor, remotely, establish a time-frame during which detectable changes in hydrate volume and stability occur, and to record oceanographic parameters known to impact hydrate stability. Attendant findings might include the ability to identify hydrate formation mechanisms in seafloor mounds, detect short-term changes within the hydrates system, identify relationships/impacts of local oceanographic parameters on the hydrates system, and improve our understanding of how seafloor stability is affected by fluid/hydrates-driven changes.

In 2009, the CMRET (Center for Marine Resources and Environmental Technology), Baylor University and Specialty Devices, Inc. (SDI) conducted a pilot survey using the DCR method to assess hydrates concentration in the shallow subsurface beneath a hydrate mound in the northern GOM. Results were very encouraging and identified shallow anomalies beneath the mound that have since been confirmed to contain hydrates in concentrations predicted, qualitatively, by the resistivities, and related to the subsurface structures only inferred on seismic data.

The team assembled to address the major questions of this project have engaged in hydrates research together and separately for many years. They have common interests in the transiency of gas hydrates and in their distributions. All members of the Gulf of Mexico Hydrates Research Consortium (GOM-HRC), they had participated in several tests using DCR methods to attempt to identify hydrates in shallow subsurface marine strata where hydrates are known to occur, at Mississippi Canyon 118 (MC118). Because MC118 had been designated by the Minerals Management Services (MMS), now BOEM, as the GOM's only Research Reserve and natural laboratory (in 2005), the group was at liberty to conduct, repeat, and amend experiments over time, as questions were answered, changed, or led to new questions.

The Center for Marine Resources and Environmental Technology (CMRET) at the University of Mississippi (UM) has long been at the forefront of the development of an *in situ* seafloor observatory. In 1999, the CMRET spear-headed the establishment of the GOM-HRC. This group of dedicated hydrates researchers investigated potential sites for monitoring and, after 5 years, selected Mississippi Canyon Block 118 (MC118) as the site for the monitoring station/seafloor observatory and began visits to the site to conduct surveys, collect samples – geological, geochemical and biological - and characterize the site. Since 2005, the group, led and administered by the CMRET, has worked to install components of a permanent monitoring station at Woolsey Mound, the cold seep/carbonate-hydrate complex at MC118. Their efforts have included developing and building sensors and tools to monitor, in real-time, *in situ* conditions on and beneath the carbonate-hydrate seafloor mound. The research effort of the GOM-HRC required the development and testing of a wide range of new technologies that have allowed Earth science to shift from making static measurements on samples and/or data collected on discreet expeditions to making continuous, *in situ*, measurements of the processes as they happen and have also accelerated the development of new instruments and experiments used in a variety of other observatory settings. For this project, we proposed to collect DCR and oceanographic data by deploying a DCR cable together with an Integrated Portable Seafloor Observatory (IPSO).

IPSO is the latest generation of CMRET's new observatory tools. Designed and built specifically for this project, it can be moved from location to location within a site and from one site to another, for periods of observation appropriate to the project. This lander was designed to provide great versatility to the project, in terms of parameters monitored, period of deployment, and site of observations.

The CMRET, has collected a wide variety of seismic and acoustic data from MC118 over the past 10 years. The data and the experience gained in collecting much of it – some with custom-designed systems – aided the 2009 effort as well as the current project. Much of the data were collected and processed in ways that would emphasize the effects of hydrates in the shallow section. We believed we had identified a signal in our Shallow-Source-Deep-receiver (SSDR) seismic data that might represent hydrates in areas where we knew - from coring and from surface surveys - that hydrates existed (Macelloni et al., 2011; Simonetti et al., 2013). We were searching for a way to extend what we were finding, laterally, and in the attempt, a way to survey for hydrates as a shallow hazard.

Study Site:

We focused our study on Woolsey Mound, a particularly well-studied example of a hydrate-bearing seafloor mound, in the northern GOM, Figure 1. Woolsey Mound is a 1 km diameter, low-relief feature in ~900m of water, pockmarked with craters and containing both active and dormant methane vents (Sleeper et al., 2006, Lapham et al., 2008, Macelloni et al., 2010). It is located in the only Research Reserve in the GOM, the site designated for the GOM-HRC's Monitoring Station/Seafloor Observatory (MS/SFO), designed and installed by the CMRET over a period of 10 years. The Mound and a fault-canyon are the predominant seafloor features of the lease block, and are located on a major slump block on the continental slope, near the landward extreme of hydrate occurrence in this region. Although site characterization is ongoing, the cold seep was selected as a natural laboratory setting due to its outcropping hydrate, abundant seeps, chemosynthetic communities, accessibility, and relatively shallow depth. In 2005, it was set aside as a Research Reserve by the MMS/BOEM so that *in situ* studies of a cold seep environment might continue even if the block were to be leased, as is now the case.

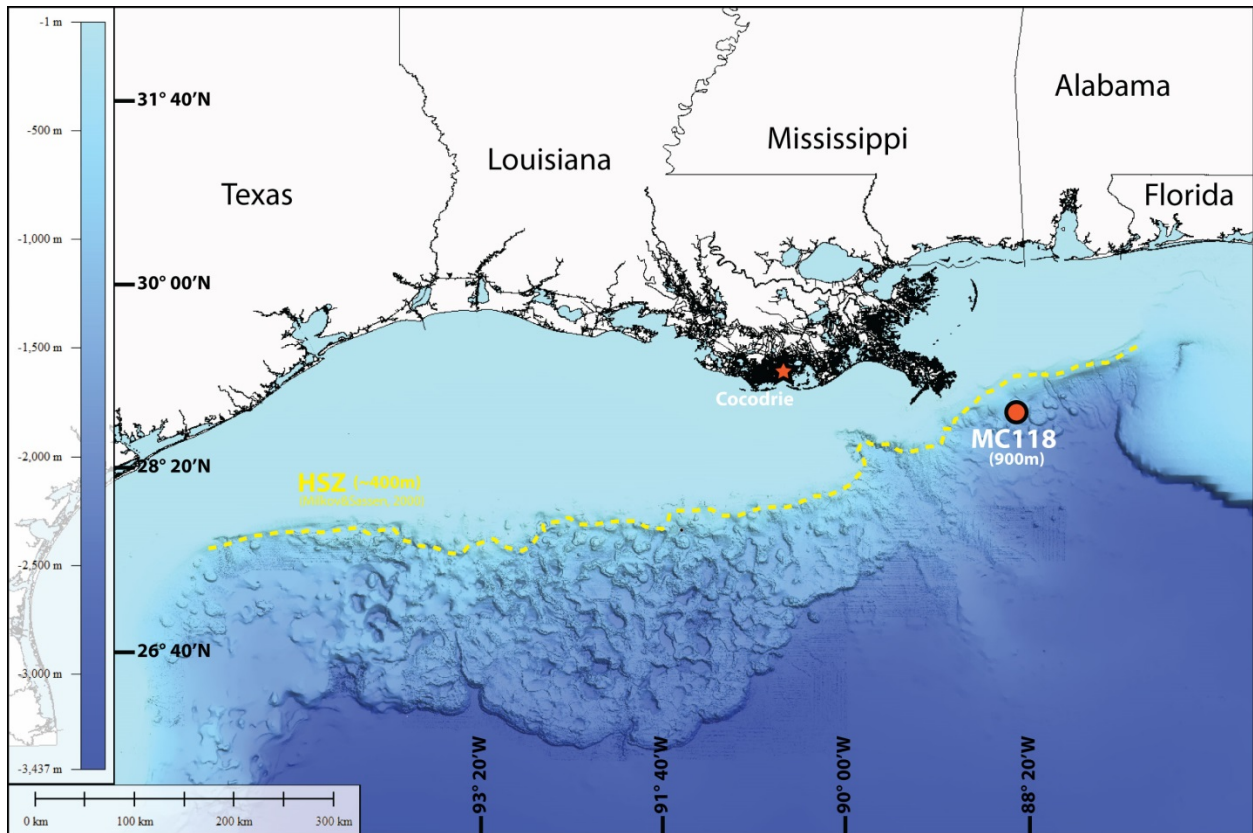


Figure 1. Northern GOM hydrate mound locations. Woolsey Mound is located in MC118 in approximately 900m of water (The top of the HSZ appears in yellow (Milkov&Sassen 2000)).

With considerable experience at this site, CMRET was able to leverage resources already in-hand to advance the study quickly. These included the 2009 DCR survey, 2005 multibeam, chirp and side-scan surveys, a more recent (2013) multibeam survey (not processed), already processed and interpreted high resolution and industry seismic data, shallow core data, a variety of video images from manned and unmanned vehicles, lander equipment and at-sea experience, from the team's research experience at Woolsey Mound. The processed multibeam and backscatter images (Figures 2 and 3) exhibit seafloor features associated with gas expulsion; areas of blanking, small faults and chaotic signal in the seismic data that reinforce these findings (Figure 4) Hydrates have been documented at the seafloor, visually, (Figure 5) and changes in hydrate outcroppings documented, photographically, to have occurred over a period of months.

The northern GOM is a perfect natural environment in which to study hydrate-bearing mounds. Salt tectonics and a massive sediment load delivered to the GOM via the Mississippi River combine to make this region a classic setting for mound formation. The concomitant presence of thermogenic gas from deep oil reservoirs and biogenic gas from the degradation of organic matter in hemipelagic sediments produces the total range of known naturally-occurring hydrates structures.

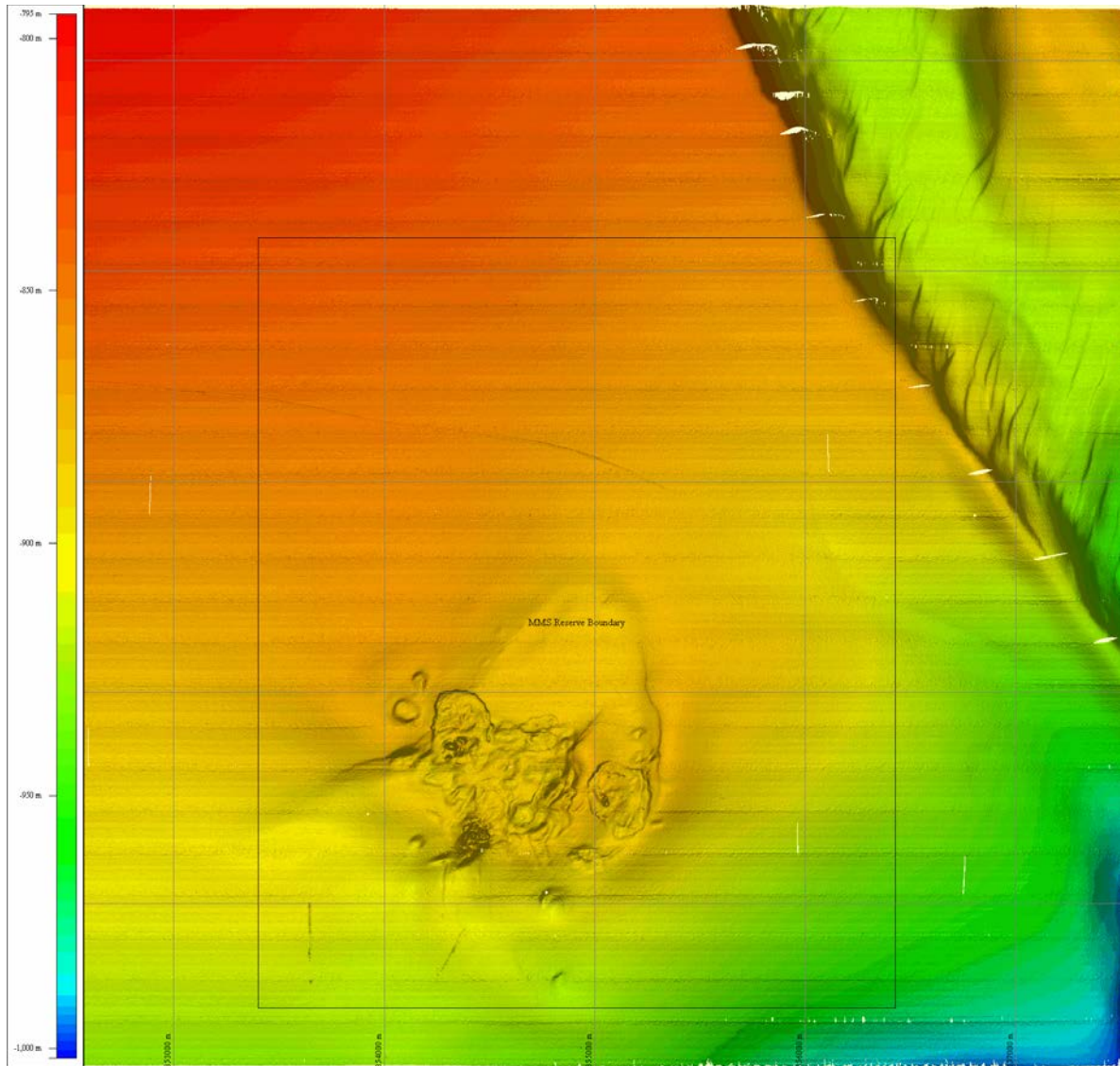


Figure 2. Seafloor bathymetry at MC118 showing 1) MMS/BOEM research reserve, 2) the carbonate/hydrate Woolsey Mound with crater complexes, sites of the natural venting of hydrocarbons , and 3) large fault to the NE that defines the western boundary of a major slump on the continental slope.

Since 2005 numerous scientific cruises, including both manned and unmanned submersibles, Remotely Operated Vehicles (ROVs), and Autonomous Underwater Vehicles (AUVs), have documented massive blocks of authigenic carbonate (Figure 5a) and hydrate slabs (Figure 5b) (Sleeper et al., 2006; Macelloni et al., 2010) at Woolsey Mound. Repeat visits to the site have shown that, in the months after the picture shown in Figure 5b was taken, the slab diminished, nearly disappeared, was replaced by a similar slab, and has now, again broken and diminished significantly. Shallow piston cores have sampled a mélangé of deformed, fine-grained sediment, mixed with large angular clasts of massive hydrate (Figure 5c and 5d).

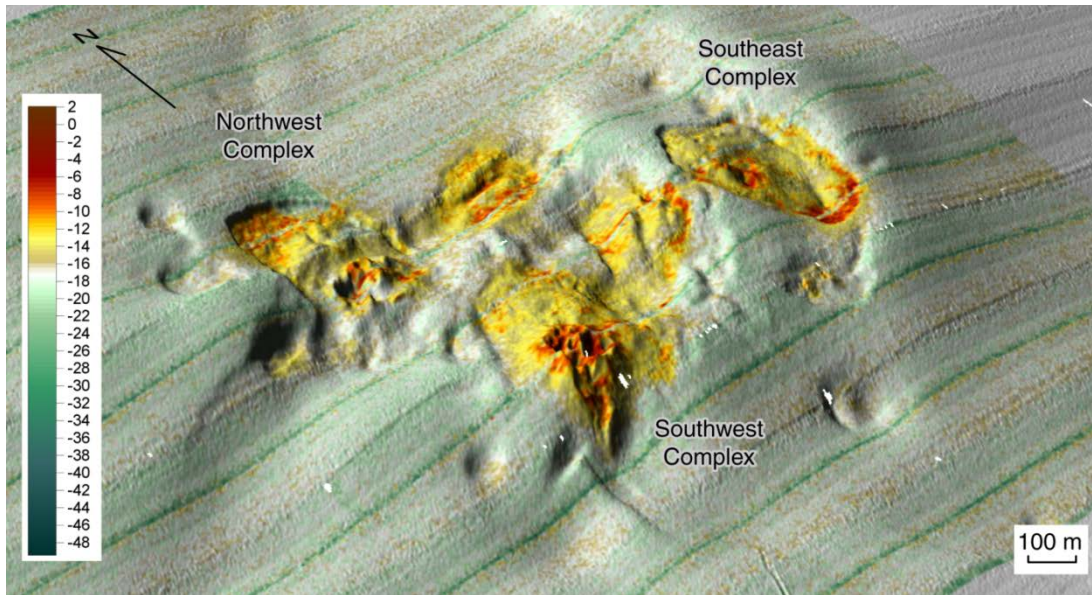


Figure 3. At Woolsey Mound, backscatter (from multibeam) data overlain onto bathymetry highlight both morphologic features and areas of exposed hard-grounds.

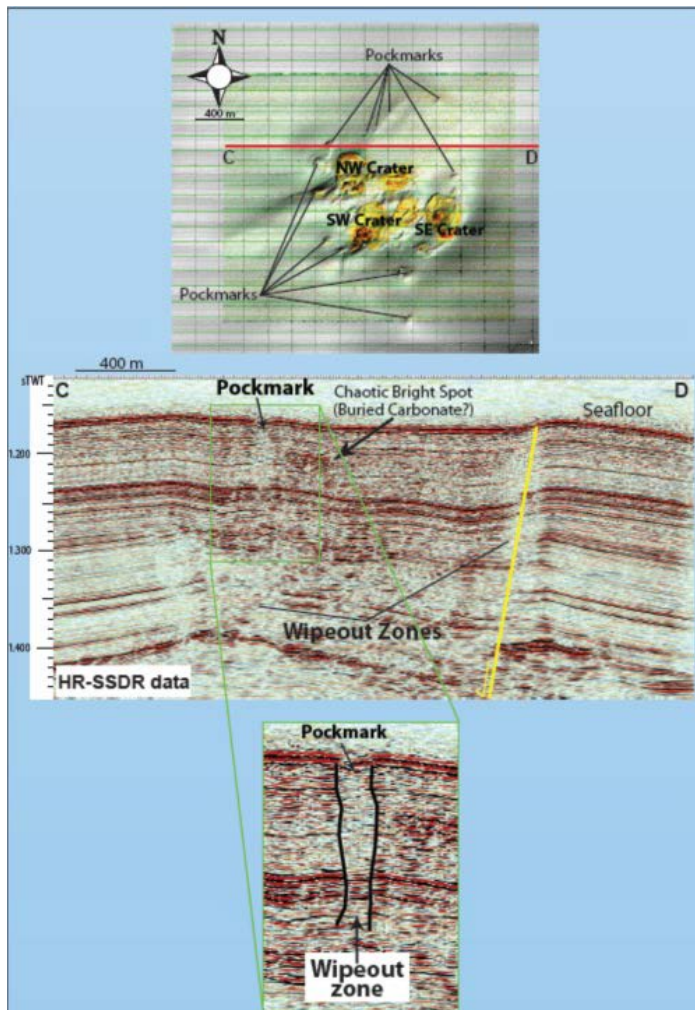


Figure 4. SSSR data show features in the shallow sub-seafloor that provide likely targets for gas hydrate accumulation. Together with seafloor bathymetry and backscatter intensity (top left), SSSR presents a picture of what is beneath the mound at MC118.

In the SSSR profile, a master fault is shown in yellow. Detail of a pockmark appears in the bottom panel. Note that wipeout zones appear variously in the profile but particularly flanking and within the highlighted features.

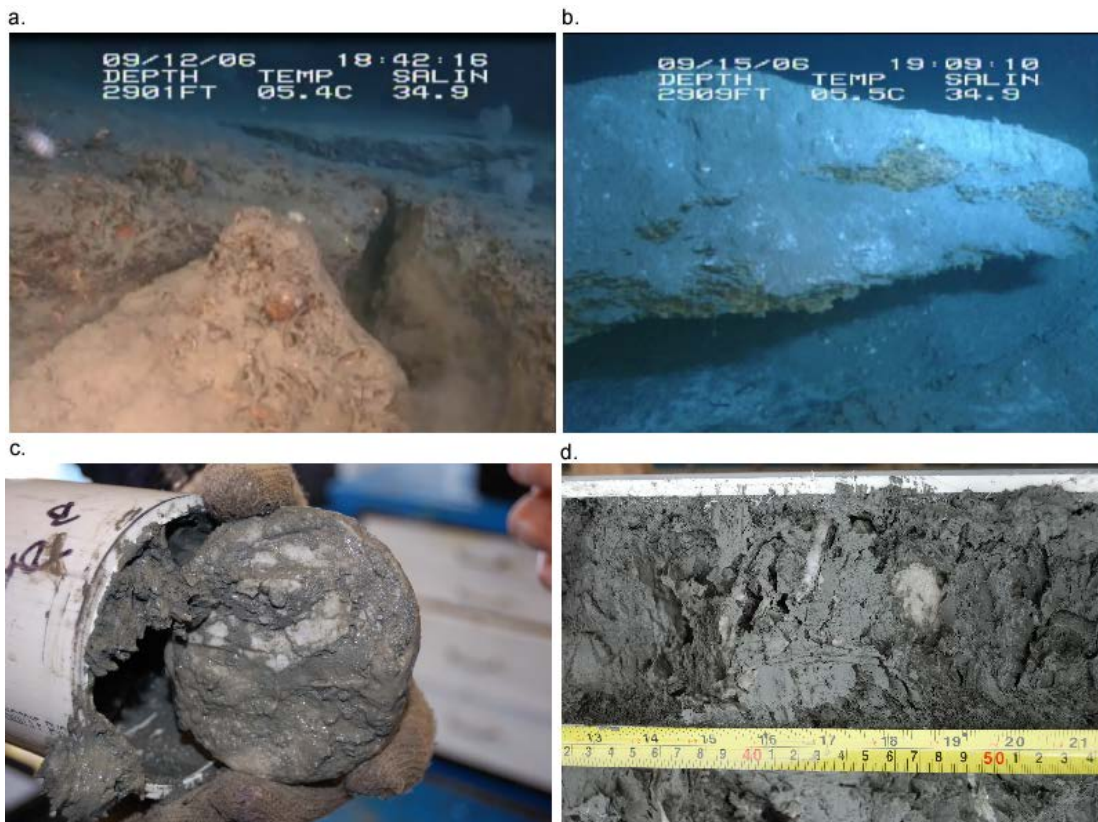


Figure 5. Near-bottom observations of Woolsey Mound, MC118. (a) Carbonate blocks on the seafloor. The foreground view is approximately 2m across. (b) Massive slab of hydrate, outcropping on the seafloor. The slab was approximately 1.5m thick and 6m long. (c) and (d) Piston core samples from the upper 15m of the sediment column, showing angular clasts of nearly pure hydrate mixed in mechanically churned, fine-grained sediment.

Previous Work:

Macelloni et al., 2012, have shown that Woolsey Mound's subsurface is part of a very complex and dynamic system, with deep thermogenic gases alternately bound in the sediment or being expelled into the water-column. AUV and ROV dives on the site, established that there is active venting and outcropping methane hydrate at the site. Massive hydrate blocks as large as 6m long, observed outcropping from the seafloor, have been documented to vanish, diminish or increase in size over a period of months. Seismic data show a complex network of faults and fractures at the site, often with no coherent reflections (wipe-out zone) beneath the mound (Macelloni et al., 2012), Figure 4.

To better constrain the hydrate distribution beneath the mound, Dunbar et al. (2010) proposed a reconnaissance survey of MC118 using the DCR method. Pure hydrate, with resistivity on the order of 20,000 Ohm-m (DuFrane et al., 2011), is essentially an insulator. Hence, massive hydrate and sediment containing significant concentrations of hydrate stand out as clear resistivity anomalies relative to sediment containing saline pore water. Unlike seismic data, which fails to "see" either gas or perfect insulators, resistivity will distinguish one from the other. In June 2009, 26 km of 2D DCR profiles were collected at MC118 by towing a 1.1-km-long electrode array along the seafloor, behind an instrument package suspended 10 to 20m above the seafloor. Profiles were collected across the mound and beyond, spaced approximately 200m apart (Figure 7).

The goal of this survey was to determine the general extent and distribution of hydrate beneath the mound. The working hypothesis for the hydrate distribution was that hydrate could be concentrated (1) within deep-seated normal fault zones that dissect the mound and access deep hydrocarbons, including gas, (2) within sill-like structures extending laterally from the faults, and/or (3) in a layer formed from free gas trapped beneath the carbonate cap covering the mound (Figure 6). Seismic data at three scales, sub-bottom acoustic profiling, shallow-source, deep-receiver single-channel seismic (SSDR), and petroleum-scale multichannel seismic, had failed to image the sub-bottom distribution of the hydrate. The seismic returns from below the mound on sub-bottom acoustic and SSDR profiles are chaotic scatter, likely from some combination of small amounts of free gas, broken blocks of limestone, and hydrate. As in other cases in which hydrate is contained in fine-grained sediment, the region below the mound is acoustically transparent on the petroleum-scale seismic data down to the expected base of the HSZ, believed to be about 200m below seafloor. The DCR method was thought to hold promise for imaging the hydrate, because hydrate is highly resistive, compared to seafloor sediments, and the DCR method is not as sensitive to small amounts of free gas as high-frequency seismic methods.

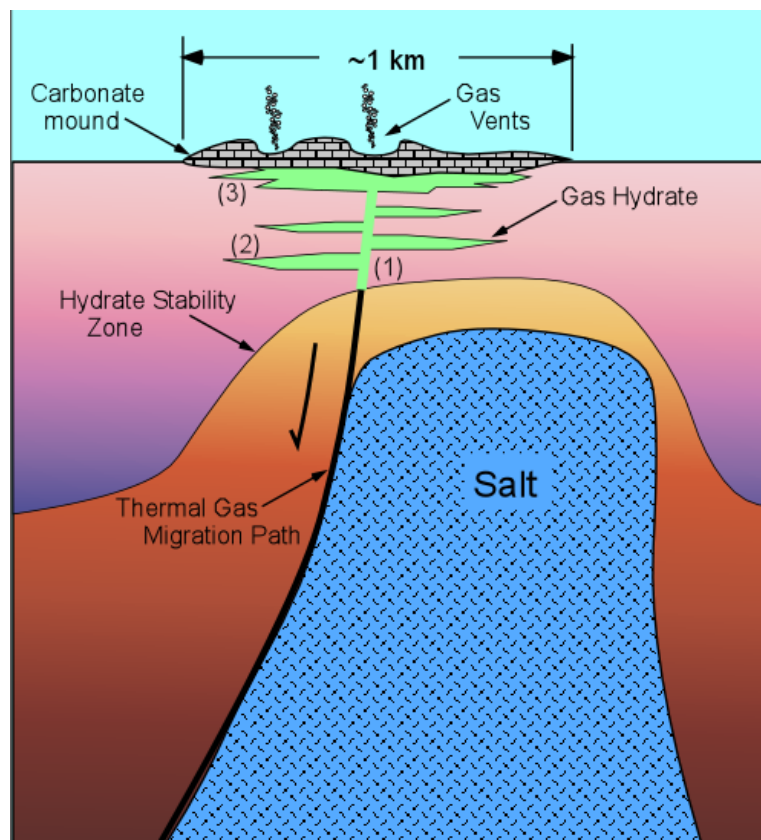


Figure 6. Schematic diagram of the Gulf of Mexico-Hydrate Research Consortium (GOM-HRC) working model of the methane hydrate distribution at Mississippi Canyon Block 118, circa 2005. Sub-bottom accumulations of gas hydrate were thought to occur, potentially, (1) within the fault zones that serve as the migration paths of thermal gas from depth, (2) within porous strata intersected by the faults, and/or (3) as an irregular layer beneath the overlying carbonate mound.

The DCR method involves injecting direct electrical current into the environment between two source electrodes, while simultaneously measuring the resulting voltage between multiple receiver electrode pairs. When combined with modern numerical data inversion routines, the method is called geoelectrical resistivity tomography (GRT). The GRT method produces 2D or 3D images of the sub-surface electrical resistivity variation. GRT is used in standard practice on land and in shallow marine settings, but had not been used in deep-marine environments prior to the 2009 survey. Two scales of DCR equipment are commercially available and are in standard use. Engineering-scale systems generally output 1 to 2 Amps between source electrodes and are used to image to depths up to 100m. Mining-scale systems generally output 10 to 20 Amps between source electrodes and are used to image to depths of 1km. Although the capacity of imaging to depths up to 1km below the seafloor would have been ideal for hydrate exploration, the plan for this first project was to start small and to scale-up the DCR system as experience dictated in later projects. The DCR system used in the 2009 survey consists of the circuit cards from a commercially available, engineering-scale resistivity instrument installed in a pressure housing suitable for use in water depths up to 1000m and a custom-made, 1.1km long electrode array. The instrument has a maximum output current of 2 amps and the capacity to measure and record voltages between up to 8 receiver electrode pairs simultaneously. The instrument is computerized, in that a list of source and receiver electrode assignments for a number of readings is uploaded to the instrument by the operator and then the instrument executes the list of readings automatically during the data collection operation without further interaction from the operator.

The electrode array used in the 2009 survey contains 56 graphite electrodes, spaced 20m apart. Graphite was chosen as the electrode material to avoid the rapid corrosion that occurs when the electrodes are used as current sources in sea-water. Having all graphite electrodes made it possible to use all 56 electrodes as both source and receiver electrodes in different array patterns for maximum flexibility and resolution. Nearly all metal electrodes erode quickly when high current passes through them into sea water. This would not have been a problem for short-duration deployments, but would have prohibited long-term, time-lapse, monitoring. The array cable contains 56, insulated-copper conductors that connect each electrode with a relay switch in the instrument through two high-pressure connectors that penetrate the pressure housing. The connections between the conductors and the electrodes are made by pressing copper rods into holes drilled into the end of the graphite electrodes and soldering the conductors onto the rods. This electrode and cable connection is then potted with urethane under pressure to prevent penetration by sea water and the corrosion that would occur as a result. The conductor bundle is impregnated with a water block material and incased in a braided Kevlar strength member, followed by a protective polyurethane jacket. The water block material prevents any water that may penetrate the jacket from moving along the cable.

For the 2009 reconnaissance survey of MC118, the DCR instrument was attached to the frame of the Station Service Device (SSD), an ROV used to service the Seafloor Observatory at MC118. The ROV provided power from its onboard battery and an emulated RS232 control link through a fiber-optic line within the ROV tow cable. The front-end of the electrode array was attached to the frame of the SSD. During the survey, and with the use of very high resolution multibeam bathymetry acquired with an AUV EM2000 system, the ROV was towed from a surface vessel 5 to 10m above the seafloor, with the 1.1km electrode array trailing behind on the seafloor. An operator on the surface vessel controlled the DCR instrument from a laptop, running an instrument emulation application that provides an interactive interface that mimics the keypad of the actual instrument. Using this interface, an operator can upload new instruction sets to the instrument, change acquisition parameters, start/stop data acquisition, and download acquired data from the instrument to the surface, all with the instrument on the seafloor.

Multiple modes of DCR acquisition are possible with this seafloor resistivity system. For the 2009 reconnaissance survey, the goal was to cover as much ground as possible within the limited ship time available. To do this, the continuous resistivity profiling (CRP) mode of acquisition was used in which the array is towed, continuously, along the seafloor, while a small number electrode patterns are repeated in a round-robin sequence. In this case, three dipole-dipole array patterns were used with two source electrodes and nine receiver electrodes distributed over total active array lengths of 220, 380, and 600m. The survey consisted of 7 profiles, totaling 26 km CRP data centered on Woolsey Mound, collected during a single dive, lasting approximately 32 hours (Figure 7).

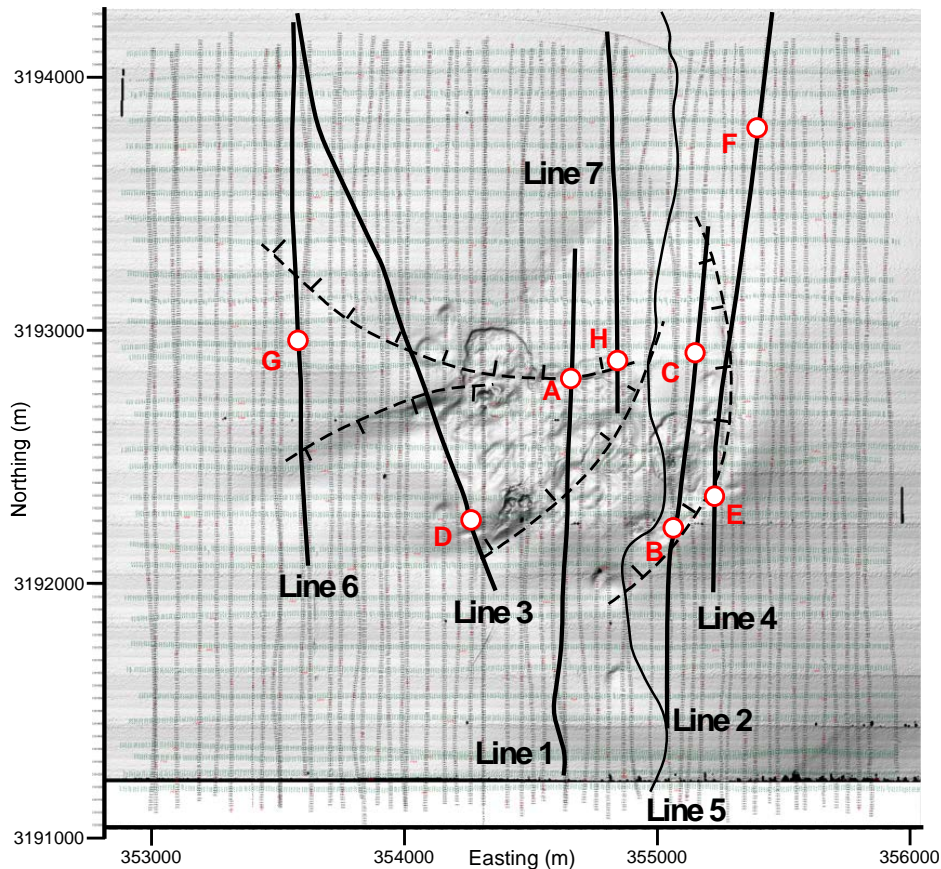


Figure 7. Shaded topographic relief map of Woolsey Mound, MC118, northern GOM. Bold black lines are resistivity track lines run at MC118 for a 2009 reconnaissance survey.; gray lines indicate the locations of previously collected high-resolution seismic profiles. The red circles mark the locations of high resistivity anomalies. The dashed lines indicate approximate traces of crestal faults previously mapped from depth to the seafloor using a combination of seismic datasets. Eastings and Northing coordinates are Universal Transverse Mercator (UTM) Zone 16.

The 2009 DCR profiles show several 100 Ohm-m resistivity anomalies in the shallow sub-bottom, suggestive of high-concentration hydrate deposits, where the profiles crossed the traces of deep-seated normal faults (Figure 8). Profile segments crossing the mound were characterized by resistivities, mostly ranging from 1 to 15 Ohm-m, with isolated pockets of 100 Ohm-m, averaging 2.6 Ohm-m within the upper 50m sub-seafloor. In contrast, segments off the mound out to distances 2 to 3 km averaged 0.66 Ohm-m in the upper 50m, with no notable

positive anomalies. Using a conservative effective media model (Cosenza et al., 2009), in which non-conductive hydrate spheres are embedded in a matrix of 0.66 Ohm-m sediment, an average hydrate concentration of 25% would be required to explain the elevated average resistivity beneath the mound compared to areas adjacent to the mound. These results suggest that high concentrations of hydrate occur within fault zones, which potentially act as conduits. Elsewhere beneath the mound, significant hydrate concentrations seemed to be limited to the first 50m below seafloor and do not extend to the apparent base of hydrate stability.

In contrast to the three working models of hydrate distribution beneath Woolsey Mount, no evidence for laterally extensive bodies of massive hydrate was found in the first 100 to 140m below the seafloor. Instead, most of the Woolsey Mound was found to be underlain by material with resistivities in the 2.0 to 10 Ohm-m range to depths of 50m below seafloor, compared to lower resistivities in regions adjacent to the mound. This is consistent with free gas and hydrate diffusely distributed within near-bottom sediments in low concentrations (5 to 10%). The exceptions occurred as small pockets of high resistivity material (20 to 100 Ohm-m) where deep-seated normal faults intersect the seafloor, consistent with high concentrations of hydrate within the fault zones or working hypothesis 1 of Figure 6 (Figure 8). However, rather than extending to the base of hydrate stability, as hypothesized, the high concentrations of hydrate within the fault zones appear to be limited to about 50m below the seafloor. Of the three proposed modes of occurrence of massive hydrate at Woolsey Mound, it appeared, based on the 2009 resistivity survey, that only the fault zones scenario was present.

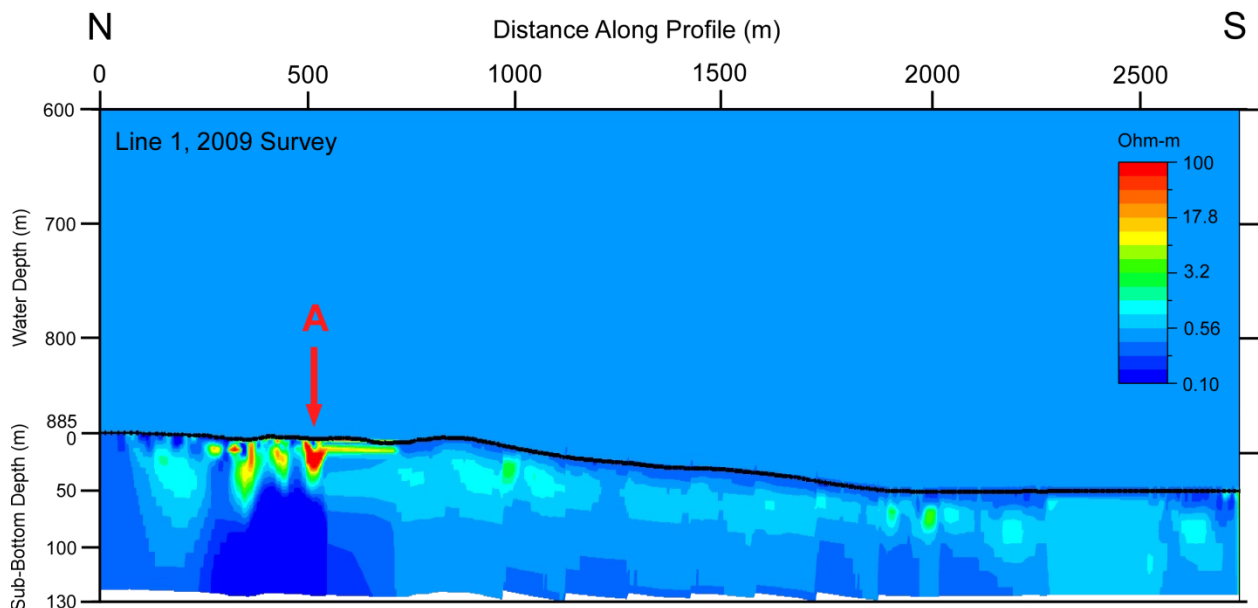


Figure 8. Example resistivity line from 2009 reconnaissance survey of MC118. The red arrow marks position of the largest resistivity anomaly observed in the 2009 survey. The location of the anomaly within the MC 118 study area is shown in Figure 7.

The 2009 survey shed considerable light on the subsurface distribution of hydrate beneath Woolsey Mound. It showed that, while present in low concentrations below most of the mound, large blocks of massive hydrate seem to be limited to the upper parts of fault zones, near the seafloor. However, two limitations of the survey left many unanswered questions, including the

pressing question of how much volume of hydrate, and therefore methane, is bound in hydrate-carbonate mounds? First, in the 2009 survey it was not possible to collect resistivity profiles directly across the most active seafloor sites, two active methane vents on Woolsey Mound. The vents contained sensitive instruments deployed by other GOM-HRC researchers. These instruments could have been damaged or disrupted by the passage of the electrode array. Hence, the sites most likely to contain massive hydrate deposits could not be investigated. Second, the line spacing of 200m used in the 2009 survey was too large to determine how massive hydrate is distributed along the fault zones. It is not clear whether massive hydrate occurs in laterally continuous lenses within the fault zones or as separate pockets of hydrate, as in a string of pearls, along the fault zones. Resolving these issues would require collecting a more complete DCR data set over the entire mound, with sufficient line density to allow 3D processing. This would require several weeks of ship time to complete, perhaps carried out over multiple cruises. However, it was also not clear whether the hydrate causing the high-resistivity anomalies in the fault zones formed in place, near the seafloor, or if it formed closer to the base of hydrate stability and subsequently moved up the fault zone in response to buoyancy forces. If massive hydrate moves up the fault zones, from deep hydrocarbon sources, it might be possible that hydrate movement could happen during a 3D survey and that such a survey would catch hydrate in the act of “migrating” along established routes. The resulting survey would then not reflect a constant volume or consistent distribution of hydrate, but rather a distribution blurred in time. For this reason we proposed the time-lapse study to determine the rate of change of the hydrate distribution beneath Woolsey Mound. The follow-on project to the 2009 survey is the subject of this report.

EQUIPMENT

The DCR system and Adaptation from Seafloor to Time-Lapse Data Acquisition:

The Seafloor DCR instrument and electrode array used to conduct the 2009 survey cannot be used on the seafloor without additional equipment. The DCR instrument housing must be mounted on some sort of vehicle or frame that can either move across the seafloor by itself, be towed through the water from a surface vessel, or placed on the seafloor and later recovered. The instrument must be powered by an external battery or through a tow cable from a surface vessel. It also must receive external control commands to operate. There is some capacity to store data on the instrument while recording, but not enough to record more than a typical field day. Hence, external data storage is required for surveys lasting multiple days.

For the 2009 survey, the DCR instrument was attached to an existing ROV that provided power and a control link to a surface vessel. In order to configure the system for long-term, autonomous recording on the seafloor, all the functionality of the ROV and surface operator had to be replaced with equipment that could be left behind on the seafloor with the instrument. The work needed to adapt the seafloor DCR system for time-lapse operation was divided between three institutions. The University of Mississippi designed and fabricated a seafloor lander, which is a steel frame that holds a large battery and mounting brackets for several pressure housings. SDI built a computer contained in a pressure housing to serve as a control computer and interfaced the computer and DCR instrument to an existing power-control/timing device called the Integrated Data Processing (IDP) unit. Baylor developed software to run the control computer and perform the operator functions during time-lapse data acquisition. The DCR instrument, control computer, and the IDP were all contained in separate housings mounted to the seafloor lander and linked by cables through high-pressure connectors in the housings. In this project, the seafloor DCR system was required to operate in two modes. In the initial phase of the April, 2015 cruise to MC118, the system was used in a reconnaissance profiling mode, controlled remotely by an operator on the surface vessel, similar to the 2009 survey.

This mode was used to collect a series of resistivity profiles to refine the selection of a profile to be monitored during time-lapse operations. To implement the remote-control mode of surveying, an existing device, the I-Spider™ or Integrated Scientific Platform for Instrument Deployment and Emergency Recovery, was attached to the lander, to provide a control link, live video feed from the bottom, and real-time positioning data for navigating the instrument package. Two-way communication between the operator at a workstation on the surface vessel and the seafloor resistivity instrument was transmitted through a fiber-optic link within a tow-cable to the I-Spider™, which transmitted the instructions to the resistivity instrument. In this way, the operator is able to change data acquisition parameters prior to data collection, trigger the start of data acquisition, monitor the quality of the data as they are collected, and retrieve the data from the seafloor instrument after the data acquisition is complete.

Once the reconnaissance resistivity data were collected, processed, and a suitable profile was selected for long-term monitoring, the lander was brought back onto the ship and reconfigured to operate in the autonomous monitoring mode without the I-Spider™ and with power provided by batteries situated on the lander. For the autonomous operation mode, the IDP was programmed to turn on power to the control computer and the resistivity instrument at one-week intervals and to leave the power on for three hours during each interval. Both the control computer and resistivity instrument were set to boot automatically when they received power. The resistivity instrument would boot and wait for instructions. The control computer would boot and automatically execute the control program written to perform the monitoring task. Each time the control program runs, it first establishes RS232 communication with the resistivity instrument. It then downloads any data files left on the resistivity instrument from the previous recording cycle to the larger solid-state storage and control computer. Once the data are retrieved, the control program erases the data from the resistivity instrument to make room for a new data set. It then transmits a set of measurement instructions to the resistivity instrument and initiates data collection. Once data collection on the resistivity instrument is initiated, the job of the control computer is complete. The control program initiates the shutdown of operating system and computer. The resistivity instrument continues to collect data until its command set has been completed and then it waits for further instructions. In the time-lapse mode of acquisition there is no mechanism for the resistivity instrument to signal the control computer that it has completed data acquisition. Instead, the IDP is programmed to leave the power on to the instrument for approximately twice the time required to collect the data and then to shut it down by cutting power.

Navigation:

To maximize the possibility of “catching hydrates in the act” of associating/dissociating, requires the ability to place packages at a selected site with accuracy as well as the ability to return to the site. Accurate navigation and referencing of seafloor features and equipment were accomplished via use of Ultra-Short Baseline (USBL) positioning system and TrakLink navigation software. The ship's location is streamed from the tech station to the bridge where the Captain benefits from the same view that the scientists have. Constant communication is maintained from tech station to bridge, enabling challenging/extended deployments and instrument emplacements. During spring 2013, MMRI/CMRET marine Systems Specialist, Matt Lowe, worked with LUMCON (Louisiana Marine Consortium) to install USBL transponders in the hull of LUMCON's R/V *Pelican*, the vessel used for this project. This effort makes the use of USBL navigation more efficient – in time – for this and following cruises, eliminating the need to calibrate sensors on every mission. to save time on every cruise executed by groups that use USBL navigation because it eliminates the need to deploy calibration instruments on the seafloor (and later recover them), mounting receivers on the ship, and the several hours required to run the survey and calibrate the receiving instrumentation.

The SSD or Station Service Device:

The SSD is an ROV designed especially for use at the MS/SFO. In order to perform a wide variety of functions, the SSD is equipped with cameras, lights, an altimeter, a 5-function manipulator arm, sonar, thrusters, USBL positioning and is battery-powered. It is deployed in a cage from a fiber-optic tether that enables researchers to receive data, live, from the seafloor as well as during dive and recovery operations. The SSD is used independently or in concert with the I-SPIDER. The SSD was used in active survey mode during the 2009 survey, towing the DCR instrument while streaming data back to the surface vessel.

The I-Spider™, Integrated Scientific Platform for Instrument Deployment and Emergency Recovery:

The I-Spider™ (Figure 9) is a battery-powered camera and light platform tethered by a fiber-optic cable to a surface support vessel. It was designed by the MMRI at the University of Mississippi with assistance from engineers at NIUST, the National Institute for Undersea Science and Technology. In addition to cameras and lights, the I-Spider™ is capable of integrating additional payloads over serial, ethernet, and fiber optic interfaces. It typically carries a scanning sonar that is used to navigate relative to seafloor equipment and bubble plumes. A tracking system with equipment mounted to the ship and I-Spider™ is used for absolute positioning. Along with the navigation sensors, a motorized release mechanism allows precise placement of instruments on the seafloor. The I-Spider™ has been used to deploy and recover a variety of marine data-collection systems. For this project, the I-Spider™ was used to provide communications with the DCR while surveying, to reconnoiter the selected deployment site for monitoring, to deploy the monitoring mode DCR-IPSO, and to recover the DCR-IPSO system.



Figure 9. The I-Spider™. This custom ROV is equipped with multiple, adjustable cameras and lights, scanning sonar, an altimeter, and USBL locator, all powered within the system. It is used to perform reconnaissance work, to deploy and recover instruments including arrays, and in concert with a working class ROV, can perform rescue missions.

The Integrated Portable Seafloor Observatory (IPSO) lander:

As described in the section on the adaptations needed to place the DCR on the seafloor for long-term collection of resistivity data, a multipurpose lander was required. The Integrated Portable Seafloor Observatory (IPSO), lander (Figures 10 and 11) was designed and built at the CMRET shop. In addition to the control computer, the DCR instrument, the IDP, and the battery to power these components of the system, the IPSO hosts the oceanographic instruments included to investigate the possible connection of a variety of oceanographic parameters to the formation or dissociation of hydrates at the seafloor. These include an Acoustic Doppler Current Profiler (ADCP) and CTD instrument that measures and records conductivity (salinity), temperature, and pressure (depth). In addition, a turbidity meter and oxygen saturation sensor were included in the suite of instruments with which the lander was equipped. With internal batteries and data-loggers, these instruments did not interfere with the data-collecting cycles or power demands of the resistivity instrument.

A LinkQuest Flowquest-300 ADCP and a SBE Seacat 16+ V2 CTD were mounted to the IPSO lander and deployed 28.856474 N, 88.484662 W from April through early September of 2014. Each logged five-minute intervals of data including standard CTD and ADCP parameters. For this study, ADCP data are plotted to show earth-oriented component velocities of each spatial axis (V_x ; V_y ; V_z), averaged velocity, and averaged signal strength. Caveat: The ADCP instrument was intended to look upward from the seafloor, and although the ADCP was set for 60 meters of range, it pitched roughly 28 degrees from vertical. The result is about 40 meters of confident range. CTD data are compared to show observations involving pressure/depth, temperature, conductivity, salinity, and oxygen saturation.

For long-term deployment, the 1100m long DCR cable was to be centered, approximately, over a target site such that oceanographic parameters measured by the instruments on the IPSO lander would reflect changes experienced in the water-column that correspond in time to changes in the measured resistivities. Gravity core, Jumbo piston core, push core, chirp, multibeam bathymetry, water-column multibeam, Shallow-source deep-receiver (SSDR) seismic, 3D industry seismic, heat-flow and many hours of video data were all used to determine likely locations at which to record resistivity anomalies.



Figure 10. The MMRI/CMRET team designed and built the IPSO lander that houses the computer communications and data storage systems for the DCR array. Instruments and batteries required for the contemporaneous collection of oceanographic data with resistivity data are also mounted on the lander. A 6-month deployment was designed to record changes in the hydrate volume beneath Woolsey Mound and the contemporaneous changes in local physical parameters.



Figure 11. The DCR cable connection to the base of the IPSO lander.

Data Acquisition, Communication and Control (atom) Computer and IDP

Specialty Devices has been working with Dr. Dunbar at Baylor University to develop and deploy a long term data acquisition, communication and control system for a DC resistivity array on the seafloor. This system utilizes a repackaged AGI Super Sting DCR system to operate the resistivity array, a control computer system to control the DCR system and previously developed Integrated Data Power (IDP) equipment which served as a system wake-up timer and power control unit for the overall system. The system goal was two-fold, to have the ability to collect real-time DCR data from the seafloor and to operate in an autonomous mode for a 6-month deployment with DCR data collected at regular intervals. The real-time mode was nearly identical to that performed previously with the SSD ROV. The long-term seafloor deployment was a new capability. SDI's contribution included design, building and housing the control computer, modifying the IDP system for this application and attending to the cables and connectors linking these systems. The IDP was modified with changes to the cabling for interface to the control computer and re-programmed for the new sampling schedule of this application. The three main pressure housings for this system were pressure tested and had their corrosion control upgraded for the long term deployment. The system was used in a towed configuration and then deployed for a long-term – 6 months or more - data collection effort.

METHODS

Cruise Activities:

Two cruises were executed to the research site at MC118. During the first, survey data were collected over the Woolsey Mound, analyzed and used to select a site for long-term deployment to monitor changes in resistivity response by recording a profile every week for as long as the batteries lasted, up to 6 months. In addition, the array was attached and anchored to a lander that housed the batteries, computers, and instruments to record oceanographic parameters that may be linked to changes in hydrate stability.

The second cruise was made to collect the equipment, to determine the value of the experiment and suitability of the equipment for redeployment. The outcome of this cruise would determine the future of the project.

Target sites for resistivity study at Woolsey Mound appear in Figure 12. The primary target site (A), is supported by the recovery of hydrate in the 2011 Jumbo Piston coring effort, by the identification of a significant resistivity anomaly during the 2009 DCR survey of the mound at MC118, by the presence of bubble plumes and by anomalously high heat flow values measured across the nearby surface trace of the fault identified in the subsurface chirp data (2005) (Macelloni, et al, 2014). In addition, analyses of multiple resolution seismic datasets support the direct communication of this fault with the crestal faults emanating from the salt structure some 600m beneath the mound (Knapp, et al, 2010, Simonetti et al, 2011). This site includes the seismic high frequency scatter signal we suspect may indicate the presence of hydrate. Site B marks the area of elevated hydrocarbon presence in a 2009 AUV survey (Camilli et al, 2009) and is the site of multiple small faults visible in chirp data as well as subsurface blanking. The heat-flow in this area is much higher than background. Area C includes the highest heat-flow recorded in 2012 after the measurement in area A. Based upon the fauna observed there (video data), this is a suspected brine pool. SDR data show a brightening 10s of meters beneath the seafloor. Area D is the area from which we first recovered hydrate in a gravity core in 2008 (Sleeper and Lutken, 2008). This site also showed heat-flow anomalies in the pockmarks in the 2012 study. The fault trace running approximately E-W through this area is the same one noted in area A that communicates with the deep crestal fault.

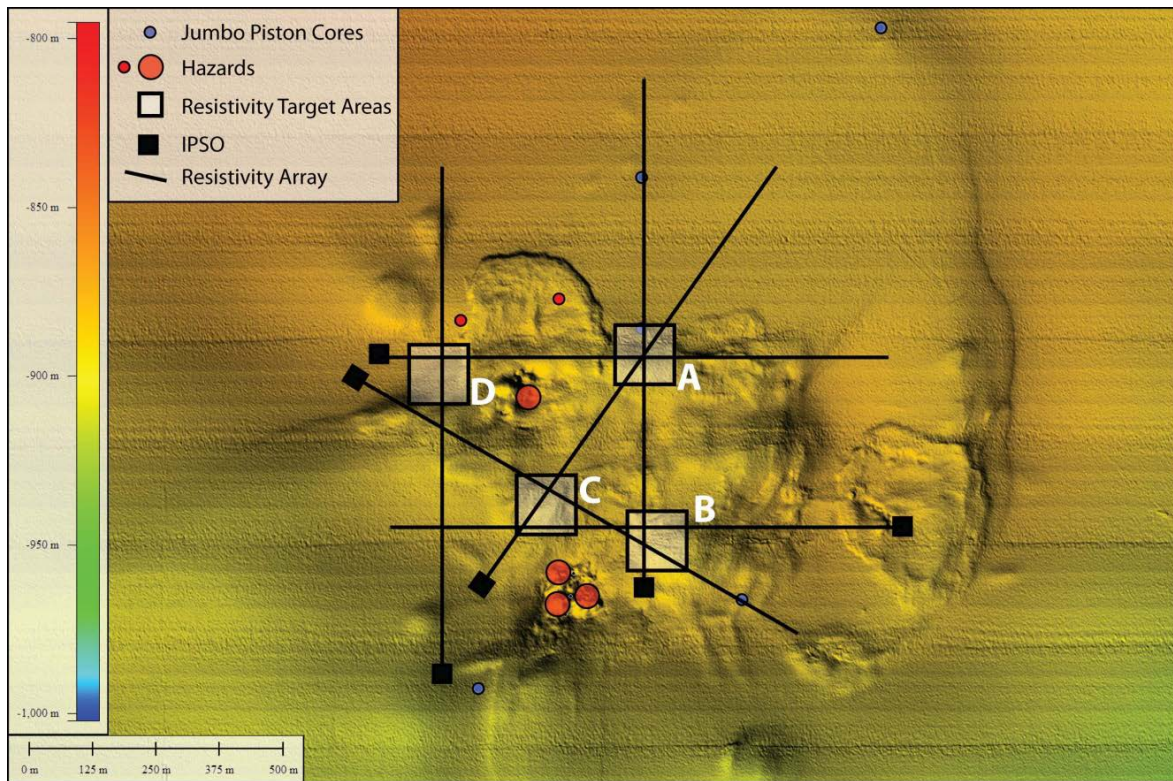


Figure 12. Proposed survey sites for the DCR study include targets and hazards on and around Woolsey Mound.

April 2014 Cruise to MC118 to deploy the DCR and IPSO system:

The plan for this cruise was to collect as many survey profiles as possible, process and analyze the data, and use the survey results to inform the selection of a monitoring site for a long-term deployment. We were looking for a site where we knew hydrates were present that might show change, over time, in their distribution in the shallow seafloor (~75mbsf). A secondary objective was to investigate possible links of hydrate formation/dissociation to changes in physical factors in the environment: temperature, depth, salinity, turbidity, currents.

The DCR cable was taped and tapered so that it could be safely deployed by spooling it onto the *Pelican's* Dynacon winch (Figure 13) then threading it through a special wide-angle shiv supported by the A-frame at the stern of the vessel (Figure 14). This lengthy and delicate procedure resulted from our need to improve upon the hand deployment used on previous DCR deployments. Once the array was in the water, it was attached to the lander (Figure 11), already coupled to the I-Spider™ on the *Pelican's* back deck (Figure 14). The I-Spider™-IPSO-DCR configuration was lowered as the *Pelican* moved into position for the first survey line. With visual contact and USBL locations via HyPack, we were able to locate all survey lines and the deployment with superior accuracy.



Figure 13. The DCR cabled array is carefully spooled onto the *Pelican's* Dynacon winch and deployed through an extra-wide shiv.

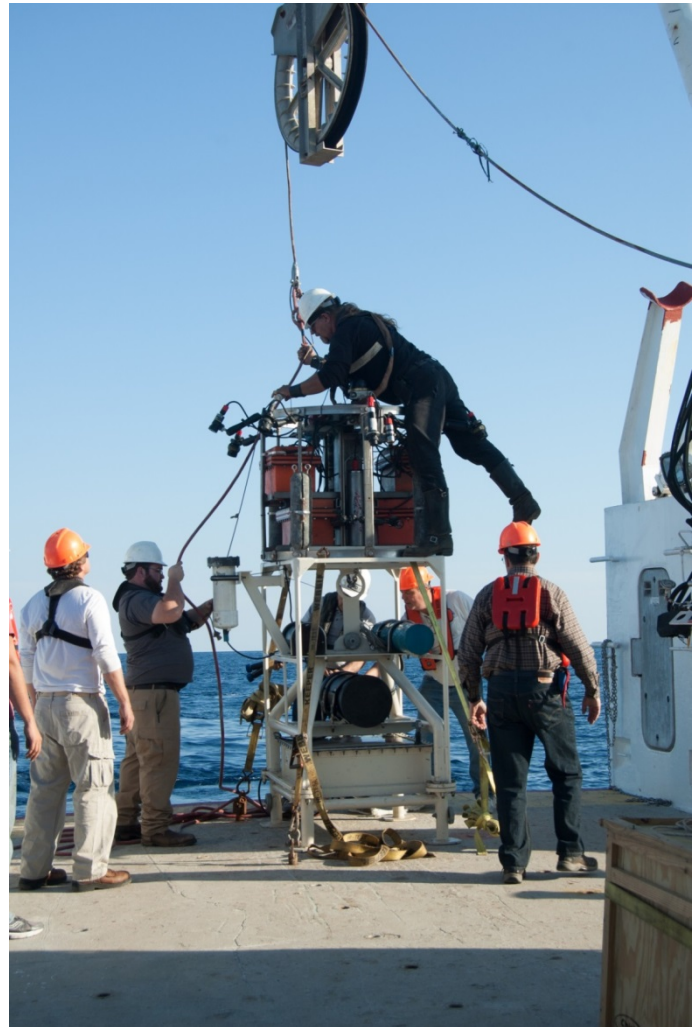


Figure 14. The fiber-optic cable is linked to the I-Spider™ DCR-array-IPSO lander assembly in preparation for deployment.

The seafloor DCR system was first configured for reconnaissance surveying to find a suitable resistivity anomaly for long-term monitoring. For this mode of acquisition, the I-Spider™ was attached to the lander. The lander and resistivity array were then towed along the seafloor by a cable attached to the I-Spider™ (Figure 14). Rather than the continuous tow method used in the 2009 survey, the array was towed along the seafloor a sufficient distance to insure that it was straight and centered on the selected target. Then the lander was lowered to the seafloor and left stationary, while a profile was collected with the fixed array on the seafloor. Once the recording was complete for a given profile, the lander was winched up off the seafloor and the array was re-positioned across a new target and the recording process repeated. The fixed-array recording mode is a slower form of acquisition on a per kilometer basis than the continuous tow method, but it produces a greater density of readings, resulting in greater spatial resolution. It also is the mode that must be used during time-lapse monitoring. Therefore, profiles collected in this stage were previews of the data that would be collected during the months of time-lapse monitoring.

Four survey profiles were collected using the fixed-array mode of acquisition (Figure 15). The data for each profile were downloaded from the seafloor instrument and processed on the surface vessel while the resistivity array was being repositioned over the next target. Lines 1 and 4 cross the mound in a more-or-less east-west direction between the two active methane vents. The goal of collecting these two lines was to determine if any large deposits of massive hydrate had been missed in the 2009 survey, as a result of having to avoid other seafloor monitoring instruments in the two vent areas. Even though the instruments had been removed, we avoided passing directly over the vents to avoid disturbing known benthic communities at those sites. Line 1 (Figure 15) shows a 220m long, 20m thick, 100-Ohm-m resistivity anomaly (Figure 16) radiating from the southwest crater. This is the largest anomaly observed in either DCR survey and appears to be an example of mode 3 of hydrate occurrence, in which hydrate forms from gas trapped beneath a carbonate cap (Figure 6). Line 4 (Figure 16) shows the same anomaly, but at a lower amplitude, possibly because it is off the edge of the causal body. Lines 2 and 3 (Figure 16) are north-south lines collected to determine if the largest anomaly observed in the 2009 study (Anomaly A, Figure 8), was still present. Prior to the April cruise, Anomaly A was selected as the primary target for long-term monitoring. Line 2, which crosses the trace of the fault approximately 150m west of the location of Anomaly A, shows a 40m wide by 10m thick, 80-100 Ohm-m anomaly, with lower resistivity (~ 5 Ohm-m) extending to a depth of 80m below it. This anomaly occurs within the westward extension of the fault zone in anomaly A of the 2009 survey. Line 3 of the 2014 survey closely followed the path of Line 1 of the 2009 survey and shows *a much diminished anomaly at the location of Anomaly A, 5 years earlier*. After Line 4 was collected, the system was brought back on deck and reconfigured for time-lapse monitoring.

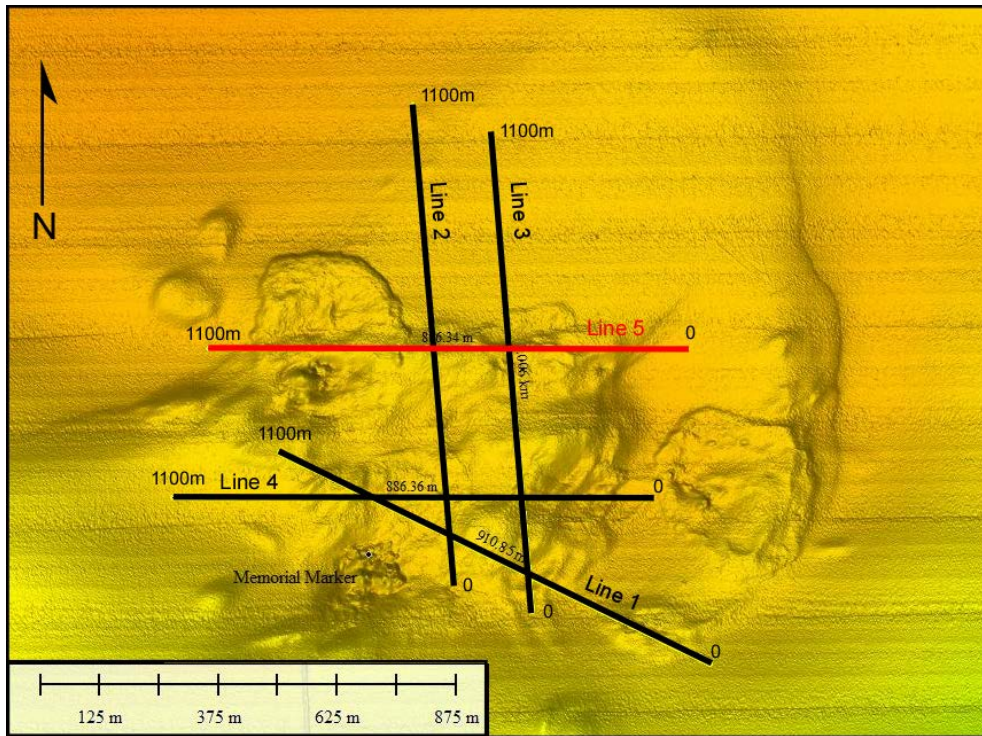


Figure 15. DCR profiles collected across Woolsey Mound, MC18, in April, 2014. Four survey/reconnaissance profiles were collected along the traces shown in black. The IPSO lander and attached DCR array were eventually deployed at the location shown in red, the lander at its eastern extreme. This deployment line lies along a fault along which bubble plumes have been observed at the seafloor and hydrates recovered (via gravity cores) from the shallow subsurface.

Of the targeting DCR lines collected in April 2014, Line 1, Figure 16, showed a large, high-resistivity anomaly, likely associated with a previously unknown massive hydrate deposit (Figure 15). Lines 2 and 3 showed smaller hydrate anomalies. However, the small anomaly on Line 3 compared to the anomaly at the same location in 2009 showed that *significant change had occurred over five years*. One of the main risks to the success of the project listed in the 2012 proposal was that an anomaly would be monitored for six months and no change would be detected. Hence, we selected a profile trending along the fault trace that contained Anomaly A from the 2009 survey as the initial monitoring target, knowing that significant change had occurred in this hydrate since 2009. The plan was to re-profile Line 1 of the April 2014 survey on the return cruise, Fall, 2014, and if the large anomaly had changed, Line 1 would be chosen for the second monitoring site. With this plan in mind, the reconfigured DCR-IPSO system was re-deployed and towed in place along Line 5 (Figure 15) and left on the seafloor programmed to wake up once per week and re-profile the line automatically. Following this deployment, we were able to confirm, visually, that the deployment was successful, with the DCR cable extended from the IPSO to the west. Although the lander was tipped, it did not threaten the functionality of the DCR or the ADCP (Acoustic Doppler Current Profiler). The I-Spider™ was recovered successfully, to be used in the fall recovery of the IPSO and DCR instrument.

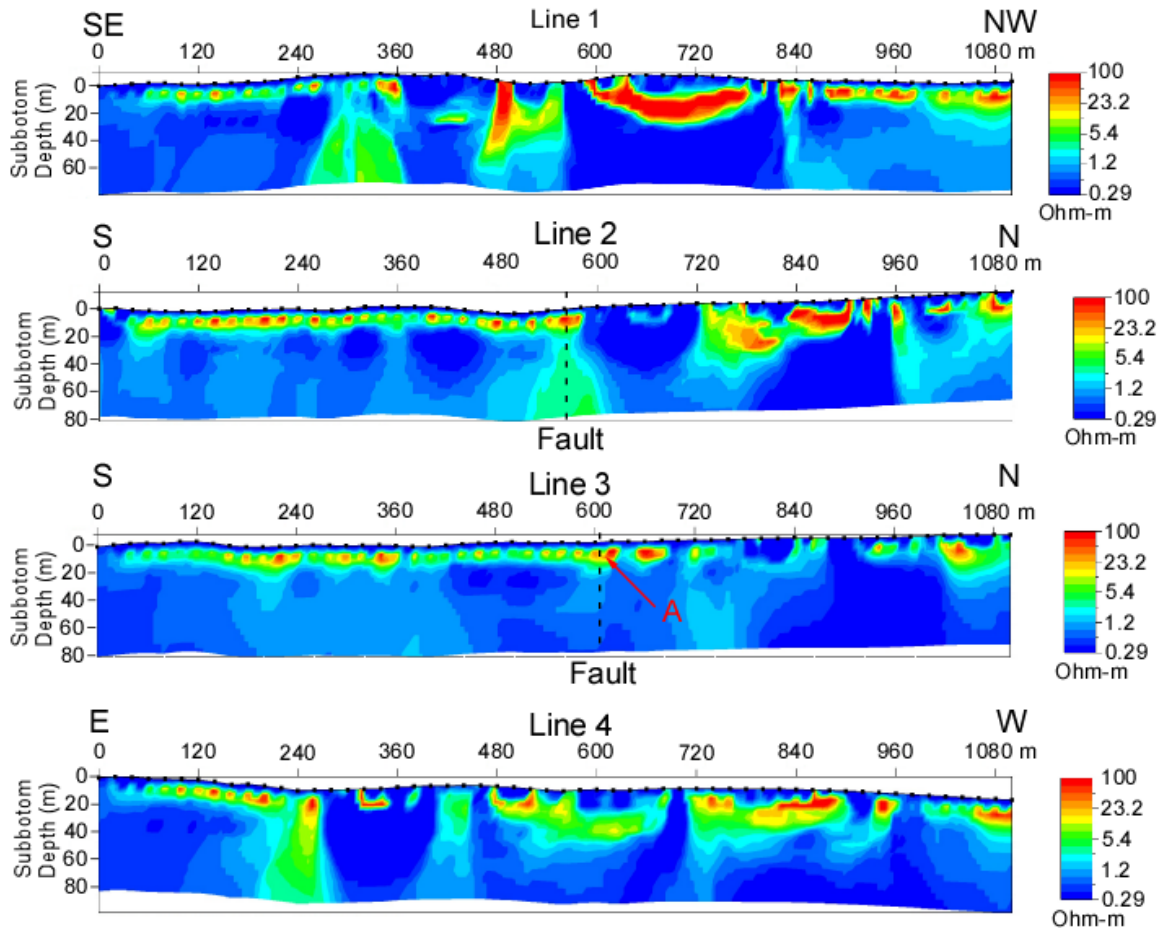


Figure 16. Initial DCR profiles collected across Woolsey Mound, April, 2014. The positions of the lines within the study area are shown in Figure 15. Vertical dashed lines on profiles 2 and 3 mark intersections of these lines with the fault trace on which Anomaly A occurs, Figure 7. The small anomaly marked “A” is in the same location as Anomaly A shown in Figure 7, corresponding to larger Anomaly A, Figure 8, from the 2009 survey.

August-September, 2014 Cruise to MC118 to recover the DCR-IPSO system:

Following the successful resistivity survey and deployment of the DCR-IPSO system at MC118, the original plan was to return to MC118, after a six-month monitoring period, to recover the equipment, and re-deploy it over a second monitoring target. Due to ship scheduling changes, the recovery cruise occurred approximately 2 months before the end of the planned 6-month deployment of the DCR system, in August-September.

We returned to the monitoring site and deployed the I-Spider™, successfully locating the lander within minutes. The I-Spider™ had been outfitted with a 4-pronged snap-grapnel, altimeter, and sonar for lander recovery (Figure 17). The lander had remained vertical throughout the monitoring period, Figure 18. Instruments, located on the north- and south-facing sides of the IPSO and the DCR cable extending to the east, indicated a recovery from the east, if possible. After many passes, we were able to achieve the ideal recovery and the DCR-IPSO system was retrieved to the Pelican’s deck.



Figure 17. Dunbar, Stoekel, and Tidwell make final adjustments to the I-Spider™ before sending it on its mission to retrieve the DCR array and instrumented IPSO lander.

Figure 18. The grapnel lands and hooks - with two prongs - the east-facing top horizontal bar of the IPSO lander.

Note oceanographic instruments on north and south-facing bars.



After the I-SPIDER was recovered to the Pelican's deck, the IPSO lander was hooked to the Pelican crane's cable and lifted from the sea to the deck (Figure 19). All instruments and pressure housings appeared to be sound. The system was removed from the deployment cage and opened in the lab of the ship. The DCR system, the IDP controller and the Atom based data logger were all recovered and in good physical condition with very little if any corrosion or damage to the housings or cabling. The battery power was determined to still be in good condition with ample stored energy remaining. Upon opening the housings all three housing were in good condition with no signs of leakage. Powering up the Atom based data logger we found it had stored data but not as much as anticipated for the length of the cruise. All functions of the Atom based computer appeared to remain functional. The IDP controller was powered up and tested and it also appeared to be in good operating condition. Further investigation revealed that only the 1st two weeks or three weeks of data appeared to have been gathered. Subsequent testing revealed that a command requesting operator input had been issued from the resistivity controller software which caused the system to stop each time the IDP requested a data set.

From the system log files, we determined that the system had worked precisely as expected through two recording cycles, meaning that the system woke up, transferred data from the instrument to the controlling computer, transferred instructions from the controlling computer to the DCR instrument, collected a profile, and then went back to sleep. However, at the beginning of the third recording cycle, 21 days after its deployment, the controlling computer woke up and tried to connect to the DCR instrument, but got no response from the instrument. This process was repeated every week for the remaining four months of the deployment. When the instrument was recovered from the seafloor, it was opened in the ship's lab. The instrument housing was found to be dry inside. However, when we tried to power-up the instrument, a "Low-Battery" message was displayed on the instrument's internal screen, with the instruction for the operator to "press any key to continue". When a key was pressed, the instrument operated normally. However, during the time-lapse deployment, there was no operator to respond to this key-press request. Hence, this message would cause the instrument to hang and not respond to the connection request from the external controlling computer. The seafloor power-supply battery was still near full charge and had plenty of power and voltage to run the instrument. The "Low-Battery" message is a feature built into the DCR instrument to prevent damage to the instrument when an attempt is made to run the instrument with an insufficiently charged battery. Hence, the "Low-Battery" message was the result of some fault in the instrument. The message had not been received during many weeks of testing in the lab, and during the survey operations prior to deployment, and yet it appeared in the ship's lab after the cruise. The fact that the instrument failed to run at room temperature in the ship's lab rules out temperature as the cause. Instead, it appears that something in the power-handling hardware associated with the instrument had changed such that this test was no longer passed. This could be the DC-to-DC converter that drops the 48 volts input from the power supply battery to the 12 volts required by the instrument. It could also be one or both of the capacitors inline with the DC-to-DC converter used to filter the startup voltage fluctuations. A third possibility is that the feature within the instrument that tests for low voltage failed. Since low-voltage had not actually occurred, a short-term fix to the problem of the instrument hanging could have been made by simply removing the low-voltage test from the instrument control software. However, this would leave the instrument vulnerable to damage, in the case that the main battery on the lander ran down during a long deployment. For this reason, the decision was made to bring the system back to shore to fix the power problem and inspect and clean the pressure housings before redeployment, later in the Fall, 2014. Once this decision was reached, none of the other tests planned for the system prior to re-deployment were performed on shipboard.



Figure 19. Recovery of the IPSO lander to the deck of the R/V Pelican was effected using the ship's crane, hooking the lift-bale once the I-Spider™ had returned the system to the surface.

Post-cruise assessments:

Battery System:

The DCR system was designed to be operated from a 12 VDC source consisting of one or two car batteries in parallel. The existence of a software detection capability to protect the system from operating on a low battery source was known and had been addressed several times in the past. In operation of the DCR system from the SSD ROV, the DCR system had been operated from a DC-DC converter which converted the 150 VDC SSD battery power to 12 VDC required for the DCR system. The system functioned without fault many times over several years.

When the DCR system was modified to run from the 48VDC available from the I-SPIDER, a similar effort was undertaken to design a DC-DC system to provide the required 12 VDC for the DCR. Following assembly of the DCR system, the control computer and the IDP, the complete system was tested through several simulated deployments without this fault occurring. The battery providing power for the system was anticipated to provide sufficient power for 6 to 7 months. The instrument was recovered some 2 months short of the planned 6 month deployment but the battery stored energy reserve indicated a much lower energy requirement during the deployment. This was determined to be a result of fewer than planned data records being obtained. The majority of the energy requirement of the system was the energizing of the electrodes during data collection. With fewer than planned data collections, the energy used was well below the planned levels.

Following the recovery the system was tested under conditions simulating those during the deployment and we were unable to find a fault in power delivery to the DCR system to cause the fault condition. The system power reserve in the deployed battery pack was not low and the connection of this battery pack to the system proved to be in good condition. We further tested the power up rise time of the DC-DC converters and found no reason for the failure to have occurred. Testing a low temperature and with higher and lower input battery voltage levels did not produce a reason for the fault to have occurred. We conclude there was a problem with the DCR system which triggered this fault warning to have been set.

Resistivity:

After the August-September cruise, we performed the tests on the electrode array on land that would have been done onboard the ship, if the re-deployment had gone as planned. The electrode array was tested for electrical isolation between electrodes and electrical continuity between the connector pins and the electrodes. The array passed the isolation test, but failed the continuity test. All 56 electrodes were no longer electrically connected to the connector pins. Two of the graphite electrodes were broken open to examine the internal connection. In both cases, the connection between the copper conductor and the copper pin forced into the graphite electrode had been broken by corrosion. Apparently the graphite electrodes are sufficiently permeable such that during the long deployment at high pressure, seawater penetrated the electrodes and corroded the connection between the copper conductors and the copper pins in the graphite electrodes (Figure 20). It would have been possible to repair the array by replacing the graphite electrodes with stainless steel or titanium electrodes, which would have prevented the penetration of seawater into the electrode. However, this repair could not have been accomplished in time for a return cruise to MC118 in the Fall of 2014. For this reason the decision was made by DOE to cancel the project at the end of December, 2014, without a second deployment of the seafloor DCR system.

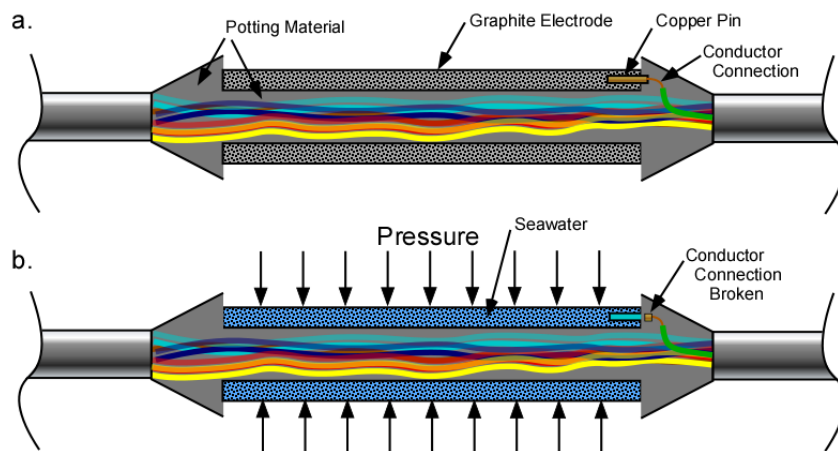


Figure 20. Cutaway diagram of seafloor electrical resistivity electrode. (a) The electrodes on the seafloor resistivity array are hollow cylinders of graphite. Each electrode is connected to one of 56 dedicated conductors, which extends from the electrode to the connector at the instrument end of the array (to the right). Conductors for all other electrodes toward the tail end of the array (left) pass through the center of the electrode. The connection between the copper conductor (green) and the graphite electrode is made by soldering the conductor to a copper pin that is pressed into a hole drilled into the graphite. The connection is then potted to hold the electrode in place and to seal the connection point from any seawater that may have penetrated the jacket of the cable to the left or right of the electrode. (b) Under long deployments at high pressure, seawater penetrates the graphite electrode and envelopes the copper pin, which rapidly corrodes when the electrode is used as a source, leading to a break in the connection to the conductor.

Oceanographic Parameters:

Although only two profiles were recovered from the DCR system, instruments mounted on the IPSO recovered oceanographic data for 21 weeks. Following recovery of the lander, data were downloaded from the data-loggers and arranged in spreadsheets for numerical and graphical analyses. While data were recorded by all instruments, some are questionable. A composite set of graphs of oceanographic data (less current data) appears in the *RESULTS* section.

Control Computer and IDP:

All housings showed no leakage and no corrosion or degradation during the deployment. The IDP and control computers systems' functioned throughout the deployment; however the data record recovered was shorter than anticipated. Following the cruise, SDI and Dunbar worked to recreate and identify the source of the shortened data record by performing tests at SDI.

All three major components of the system survived the deployment with no leakage or other detrimental effects of the deployment and should have survived the next deployment well. The only exception to this was some minor corrosion evident on the DCR pressure housing. This housing was designed anticipating only short-term deployments and had been modified to improve its resistance to corrosion for these 6-month deployments. Replacing sacrificial anodes and recoating the surfaces would allow continued 6-month deployments.

Significant effort was required to recover the system from the seafloor and a plan to simplify the recovery could be implemented should the system be redeployed. This was due to the requirement to physically attach to a small target on the structure. Deployment of ground tackle on the sea floor opposite the electrode array could have made recovery a quicker task.

Following recovery of the system, it was determined that it had not collected a complete data set. There appeared to be two of an anticipated 18 datasets stored with a possible third data set remaining in the DCR system memory. The reason for the missing datasets was determined to be the result of a DCR system request for an operator response to continue data collection.

The DCR system was designed to be operated from a 12 VDC source consisting of one or two car batteries in parallel. The existence of a software detection capability to protect the system from operating on a low battery source was known and had been addressed several times in the past. In operation of the DCR system from the SSD ROV, the DCR system had been operated from a DC-DC converter which converted the 150 VDC SSD battery power to 12 VDC required for the DCR system. The system was used successfully many times over several years without fault.

When the DCR system was modified to run from the 48VDC available from the I-SPIDER, a similar effort was undertaken to design a DC-DC system to provide the required 12 VDC for the DCR. Following assembly of the DCR system, the control computer and the IDP, the complete system was tested through several simulated deployments without this fault occurring. The battery providing power for the system was anticipated to provide sufficient power for 6 to 7 months. The instrument was recovered some 2 months short of the planned 6 month deployment but the battery stored energy reserve indicated a much lower energy requirement during the deployment. This was determined to be a result of fewer than planned data records being obtained. The majority of the energy requirement of the system was the energizing of the electrodes during data collection. With fewer than planned data collections, the energy used was well below the planned levels.

Following the recovery, the system was tested under conditions simulating those during the deployment and we were unable to find a fault in power delivery to the DCR system to cause the fault condition. The system power reserve in the deployed battery pack was not low and the connection of this battery pack to the system proved to be in good condition. We further tested the power-up rise time of the DC-DC converters and found no reason for the failure to have occurred. Testing a low temperature and with higher and lower input battery voltage levels did not produce a reason for the fault to have occurred. We conclude there was a problem with the DCR system which triggered this fault warning to have been set.

RESULTS

As can be seen in the composite graph, Figure 21, the conductivity (salinity) sensor returned erratic data for the initial 17 days of the deployment. The oxygen saturation shows a similar pattern; however, as it is a derived (from the conductivity sensor) entity, this is not a surprise. Something happened on or about day 17 that resulted in the sensor returning normal values. This 17-day time corresponds almost exactly with the period of time that the resistivity array was collecting data. Pressure, depth, and temperature appear normal though temperature does decrease slightly following the event in the conductivity.



Figure 21. Composite of oceanographic data collected during the 4.5 month seafloor deployment from April 14 through September 3, 2014.

ADCP data were collected over the entire 21 weeks and x- (east-west), y- (north-south) and z- (vertical) components broken out and plotted against the CTD data. These plots for the weeks over which resistivity data were recovered appear as Figures 22, 23, and 24.

ADCP velocity data fall below 0.6 m/sec. A North-South component (V_y) frequently shows more water movement over the entire vertical range. This movement mimics the daily tide somewhat in frequency but certainly not in phase. There also exists an intermittent pattern of water

movement found only near the instrument, in the range less than ten meters from it. Figures 21, 22, 23, and 24 all show the unfortunate erratic conductivity/salinity return from the CTD. This reading, reliably in the 34-35psu (or ppt) range at Woolsey Mound and at 885m water depth, starts well below this at ~30psu, falls suddenly then rises to a reasonable level of ~35psu on day 17 of the deployment. We puzzled over this troubling result and decided to contact others with expertise in CTD data. After consulting the manufacturer of the instrument and several CTD operators and data experts, we are left with possible explanations that include mistaken start-up settings, fouling of the sensor, failure of the pump, a lens of fresh water. The deployment settings were set by an experienced technician and an engineer together, checking each other's work, so the first seems unlikely. There was no oil noted on the water's surface, nor was there active bubbling at the deployment site, so fouling by venting hydrocarbons, while still a possibility, seems unlikely. We had visuals for the deployment which show it to have been very clean. Figure 18 shows the position of the lander at recovery and while we feared the possibility that the lander, deployed at an angle of 28.5° might have fallen over, we were pleased to see that it had not. A CTD cast was made from the research vessel quite near the deployment site prior to the survey component of the deployment cruise, about 35 hours prior to the lander deployment. This cast returned reasonable conductivity and O₂ values. Although this information cannot unequivocally rule out the possibility of a fresh water lens, it argues against it, not only in time but in location, primarily vertically. Since fresh water is less dense than salt water, fresh water moving into the bottom of the water column, mid-slope, is extremely unlikely. Another possibility is that the instrument collected fresh water higher up in the water column and that the instrument failed to purge it in 17 days. This argues that the pump failed and then "recovered." While unlikely, this is not unheard of as batteries are known to operate intermittently under high pressure. This appears the most likely scenario and, unfortunately, renders the early conductivity data untrustworthy.

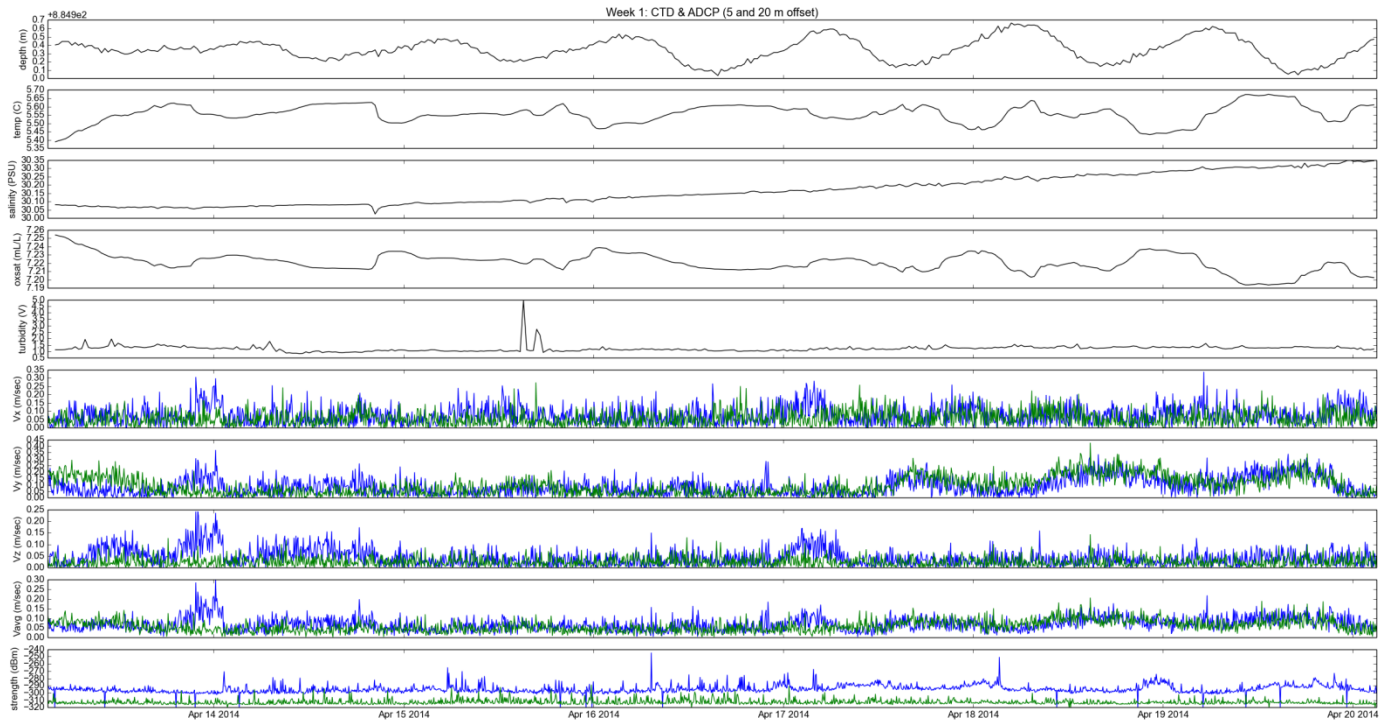


Figure 22. ADCP components x (east-west), y (north-south), z (vertical), plotted in near-range and in 20m range, together with CTD data, week 1 of deployment.

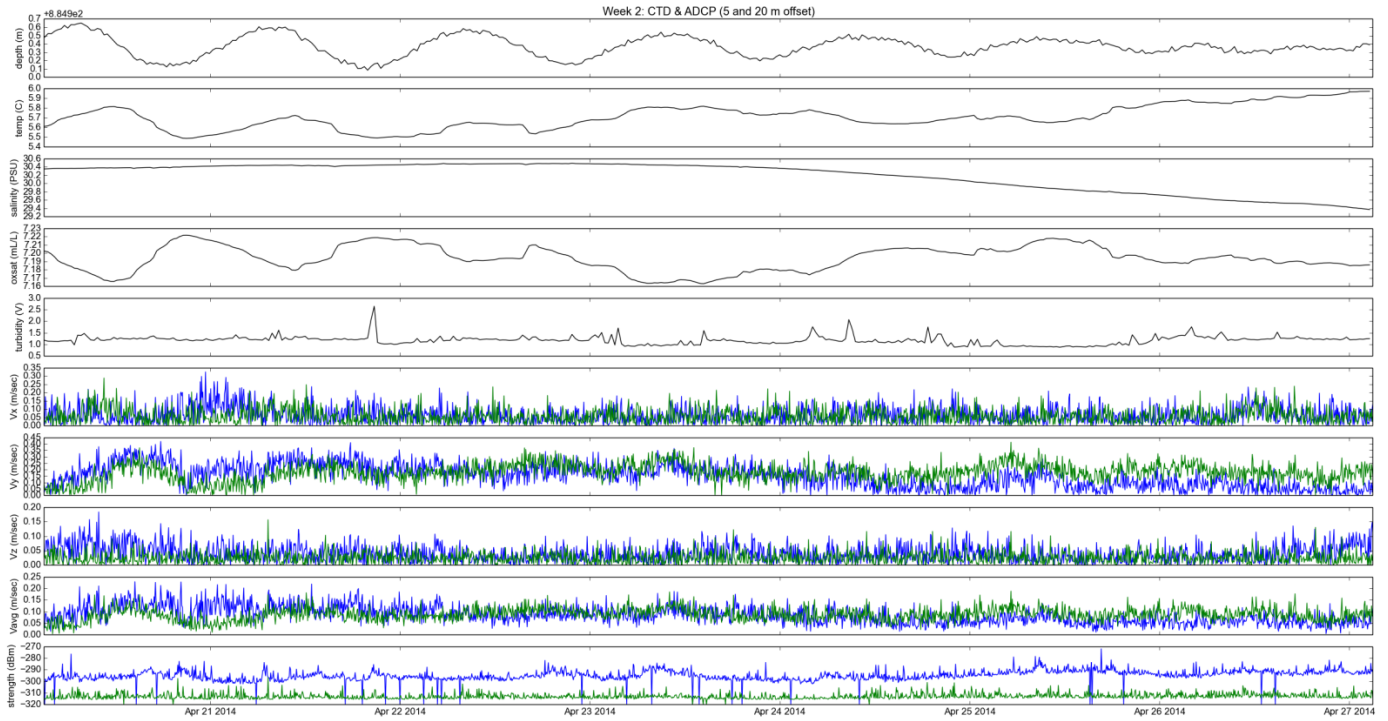


Figure 23. ADCP components x (east-west), y (north-south), z (vertical), plotted in near-range and in 20m range, together with CTD data, week 2 of deployment.

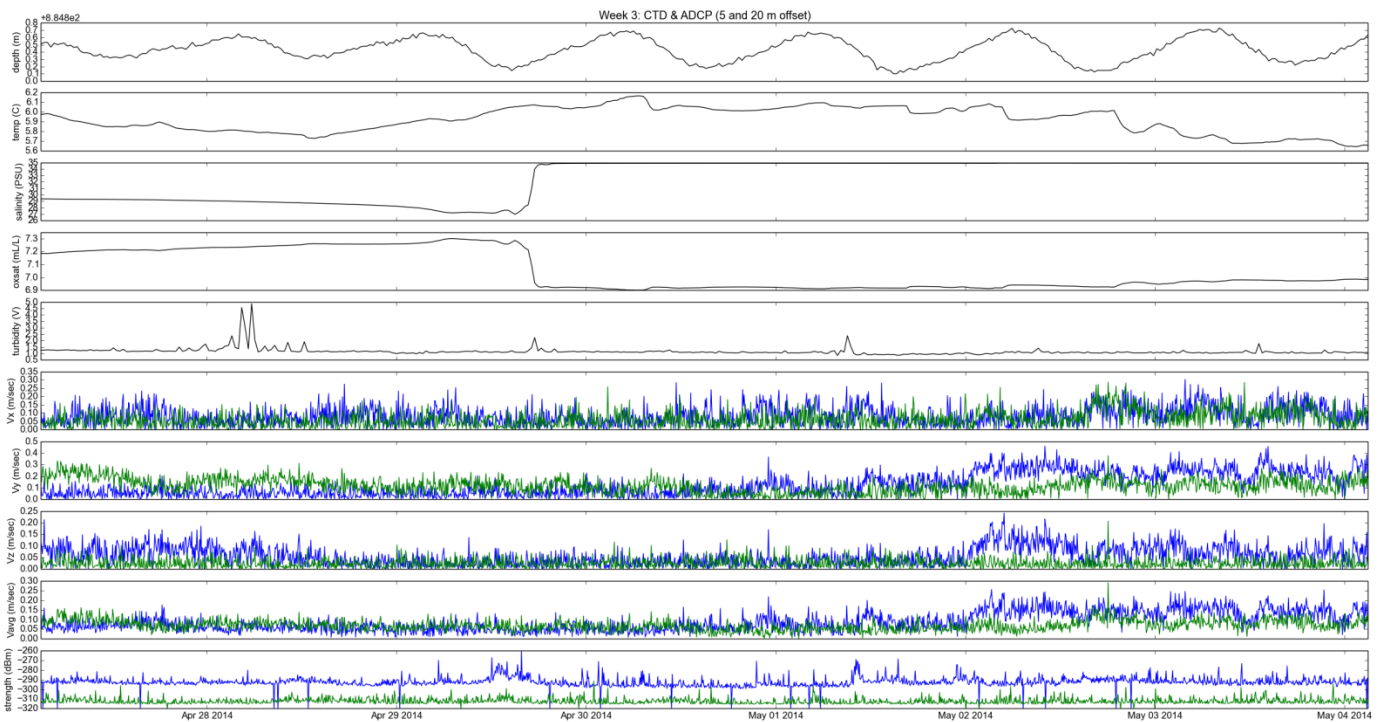


Figure 24. ADCP components x (east-west), y (north-south), z (vertical), plotted in near-range and in 20m range, together with CTD data, week 3 of deployment. Note “event” recorded in the conductivity and oxygen saturation values. Possibly “cleansing” of the sensor is related to the turbidity event of April 28.

After the cruise, the two DCR profiles that were recorded were processed in time-lapse mode using the commercial resistivity inversion package EarthImager2D™. The resultant resistivity change image, Figure 25, shows that **even within the short span of two weeks, significant change in the distribution of high resistivity anomalies associated with hydrate concentration changed**, resistivity increasing by 200% within a 60m wide zone, from near the water bottom to 40m below bottom, east of the intersection with Line 1 of the 2009 survey and Line 3 of the April 2014 survey. In contrast, relatively little change occurred in the western portion of the study area, near the Northwest methane vent and crater (Figure 25). This suggests that massive hydrate may form in small, isolated pockets at different times and locations along the fault. There were also smaller zones in the eastern part of the same profile where resistivity decreased between week 1 and week 2. However, the amount of decrease was less than increase and zones in which decrease occurred were smaller, indicating a net increase in hydrate within the fault zone in this one-week period. A longer time-lapse sequence would be needed to see if formation occurs in the same location for months or years, or if the focus of hydrate formation switches rapidly from one location to another long the fault.

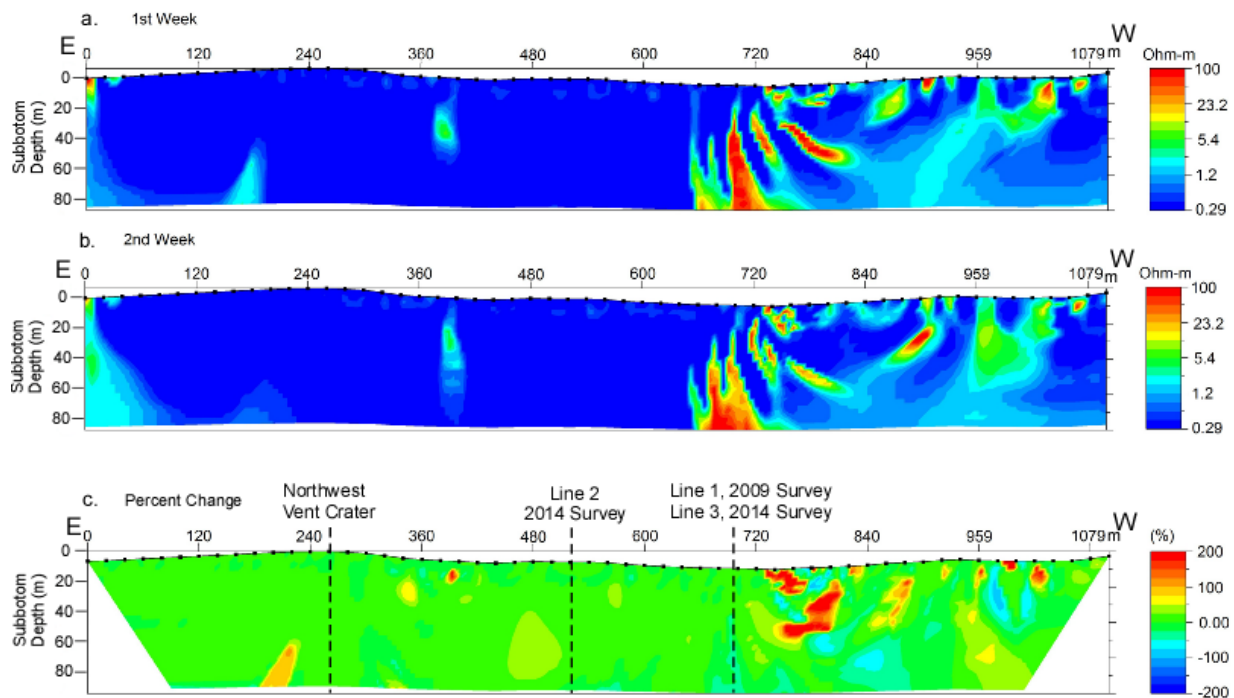


Figure 25. DCR Time-lapse profile. The line of section corresponds to Line 5, indicated in Figure 15. (a) Profile collected on April 18, 2014. (b) Profile collected on April 26, 2014. (c) Percent change in resistivities between first and second week. Positive percentage changes correspond to increases in resistivity between the first and second week; Negative percentage changes correspond to decreases in resistivity between the first and second week.

DISCUSSION

The failure of the CTD instrument to return conductivity and oxygen data that we can believe during the very time that the resistivity instrument returned such excellent data dealt a severe blow to our hopes to be able to tie oceanographic data to hydrate formation and dissociation. It was our hope that hydrate “events” might show up as geochemical events if the lander and its instruments were within range of the event. While the conductivity and oxygen data cannot be

trusted prior to day 17, the ADCP data can. However, the range of detectable events in the ADCP data appears well below its distance (~500m) from the hydrate anomalies. Had the lander been at the eastern rather than the western end of the DCR array, we should have experienced a better intersection of datasets. The current data rendered by the ADCP do tell us that for this deployment, regional trends were experienced primarily in the north-south direction.

Figure 26 presents turbidity data together with current data. Turbidity data can be seen to correspond to current velocity data, but with no major events in the early days of the deployment.

The DCR profiles, though different, share some important characteristics. The significant anomalies occur in the western portion of the study area (refer to Figure 15) and, as shown in Figure 25, access the seafloor only in the western half of the profile. Figure 27 shows the SSDR profile that most closely approximates the DCR monitoring profile. When the DCR profile is overlain onto the SSDR, some interesting generalities appear. Although the SSDR profile and DCR profile do not correspond exactly to the same pass over the mound, the overlay reveals close proximity of several features.

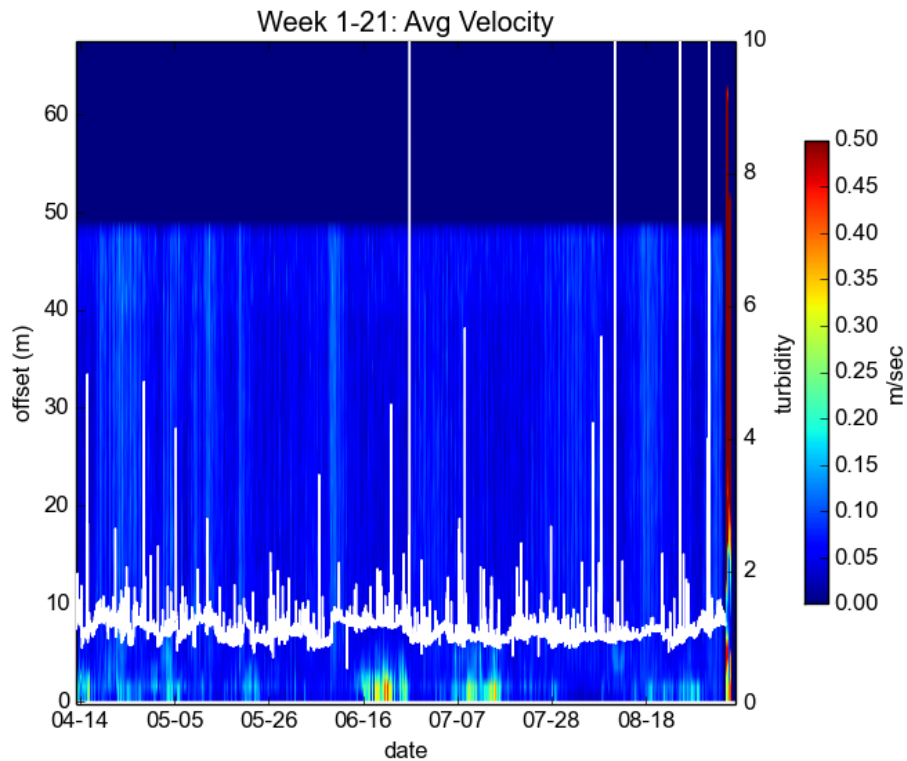


Figure 26. ADCP average velocity highlighting near-range net water movement. Turbidity (in white) is plotted over the current velocity.

An important open question and scientific challenge in near-bottom gas hydrates assessment is how gas hydrate is distributed throughout the sediment fabric. Efforts to understand how hydrate clathrates and host-sediment grains mix and interact comprise much ongoing research effort. Some of the numerous possible grain-to-grain morphologies include the following scenarios which occur in some gas-hydrate systems:

- uniform hydrate dissemination throughout available pore space,
- alternating layers of hydrate-rich and hydrate-free sediments,
- load-bearing clathrates,
- thin sheets of hydrate filling laminae and fracture voids.

Each of these grain-to-grain morphologies requires a different rock physics model to relate volume concentration of gas hydrate in deepwater sediment; and seismic attributes are often unable to resolve this ambiguity because these are compositional anomalies and can produce non-unique seismic response (i.e. seismic blanking, high amplitude patches, etc.) For example, in the upper (SSDR) panel of Figure 27, the eastern portion appears to be much less disturbed than the western portions, with reflectors more horizontal, more clearly defined and more regular. This can represent the normal layer cake sedimentation of the Gulf of Mexico continental slope. In contrast, the western portion of the profile appears to be highly disturbed and to exhibit both blanking and patches of high amplitude anomalies at ~40mbsf over much of the profile. Reflectors are broken and often subparallel. Seismic data, in this case, suggests the presence of gas pockets and buried, high reflectivity bodies such as carbonate crust/nodules, in any case an ambiguous scenario. In comparison, the DCR profile displays almost no anomalies in its eastern portion while it is riddled with anomalies in the west. The very small anomalies in the east do not reach the seafloor. In the west, many do. Numerous vertical fluid-flow paths extend from considerable depths and reach the seafloor across the northern Gulf of Mexico. Some of these vertical conduits are fault planes; some are fluid/gas expulsion chimneys. While we do not show the proprietary deep section seismic data, we know that this fault, approximated by the DCR profile, extends to depth, providing access to the seafloor for hydrocarbons migrating along this faulted section. Each type of fluid-flow feature allows deep thermogenic methane to migrate upward and enter the gas-hydrate stability zone where it becomes entrapped in hydrate cages. Many of these vertically oriented faults and gas chimneys are detectable with conventional towed-cable marine seismic methods, but seismic data cannot “tell” the composition of these structures. Our DCR data prove that there is a particularly compelling correspondence between resistivity anomalies that reach the seafloor and the small faults evident in the SSDR profile, western portion. Therefore if such sub-seafloor structural features are observed in water depths that sustain gas hydrate, there is a good possibility a gas-hydrate accumulation is genetically related to the faults and/or chimneys. Were we to have made additional deployments, the oceanographic instruments would have been deployed in this area where hydrate “activity” might be reflected in the parameters measures at the seafloor.

Suggested System Modifications

A very large majority of a deployed system can work perfectly but one or two problems can spoil an otherwise stellar effort. We feel that if a very few issues could be addressed, the system would be much improved.

First, the CTD should be returned to SeaBird for QA/QC. We have been in communication with the manufacturer, have collected test data and have run repeat tests with the instrument running neither to our satisfaction or theirs. This project was the CTD’s first field test after performing on the bench. We should have run sea trials to prove its reliability.

The resistivity array should have the graphite electrodes replaced with sacrificial metal electrodes. These electrodes can be replaced, individually, in the field. Sacrificial electrodes can be constructed with sufficient material that a 6-month or longer deployment can be accomplished without failure to function or damage to the cable. Replacement electrodes can be designed to be quickly replaced on deck between deployments.

The battery fault issue can be addressed by removing the battery fault line in the system code, further investigation into the reason this fault was triggered or adding the capability to the control computer software to automatically answer the DCR question.

The simple solution is to remove this fault detection from the DCR code. The cost of a deployment and recovery cruise makes the much lower cost of potential damage to the DCR system inconsequential.

Alternately further testing and visibility into the conditions that cause this condition to be triggered can allow the power source to be designed to prevent the fault from triggering. In the testing process both before and after the deployment, it had been understood that this fault was triggered by a low battery voltage level. Although we could not replicate this fault in lab testing without having a truly low battery voltage, it may be that the timing of this fault detection has an effect on the determination of the existence of a fault. Variable voltage rise rates were implemented with the addition of capacitors to the output of the DC-DC converters and the rise rate was monitored. A fault mode was still not recreated in lab conditions.

The command request issued was one that involved asking if the battery status was acceptable to continue operations. We believe this request should either be deleted from the operational code or a delay start up relay be installed in the resistivity system to remove the resistivity system's capability to test this battery status until the system DC-DC converters are up and running a sufficient time to prevent this request from being issued. Short of this software issue the system electronics functioned as designed throughout the deployment period.

CONCLUSION

The current project clearly adds significant new information to the knowledge-base of hydrate distribution beneath carbonate-hydrate mound complexes. The 2009 DCR survey suggested that high-concentration hydrate only occurred in small pockets near the seafloor, within faults. Sheets of hydrate filling laminae and fracture voids up to massive hydrates dykes filling fault planes is the most realistic scenario in the development of hydrates mounds. This would imply that there is far less hydrate beneath the mound than expected. However, the first pre-deployment DCR profile during the April 2014 cruise showed that, as previously suspected, large sill-like hydrate structures do exist beneath the mound. Also, the third pre-deployment profile, which closely repeated Line 1 of the 2009 survey, indicated that the largest anomaly found in the 2009 survey had *reduced in size in five years*. Hence, ***the hydrate distribution beneath the mound changes over periods of several years***. The two-week, ***time-lapse monitoring deployment established that the hydrate system undergoes detectable changes on the time scale as small as one week***. Hence, future monitoring efforts should be directed to repeat profiles with at least that frequency, if not greater.

The main aspect of the hydrate system beneath Woolsey Mound remaining unresolved is the mechanism by which massive hydrate occurs. The question is, does the hydrate form in place from the movement of methane-saturated water to near the seafloor or does it form at greater depth below the seafloor and move by buoyancy forces to the position in which it is found? The fact that the hydrate causing anomaly A of the 2009 survey had largely disappeared by 2014 indicates that the hydrate was out of chemical equilibrium in that location. This suggests that it was allochthonous. It was hoped that in a long time-lapse record at the site, one could watch either the gradual growth of a hydrate body in place and/or the gradual movement of a pre-existing hydrate bodies from depth, toward the seafloor. The resolution of this question remains for future work.

Accomplishments:

In spite of failures associated with the performance of the CTD instrument, the insulation material for the nodes and the specifics of the software for the remotely operated computer, there are a number of accomplishments of this project which should be noted and which provide points from which to advance the study of marine gas hydrates that form near/within mounds:

1. The development and deployment of the DCR-IPSO lander marks an achievement in deployment capability. For the first time, we deployed lander-supported equipment with a seafloor array using the I-Spider™, a heavy-duty ROV with eyes on the seafloor. We chose the seafloor site “on the fly” and with good knowledge of the environs of the deployment. We made a video recording of this.
2. We accomplished a resistivity survey in deep water, using the I-Spider™ as the power and visuals provider as well as the deployment vehicle.
3. We recorded marked changes in resistivity in the shallow subsurface at the study site. The survey data prove that these changes occur over a period of 5 years.
4. **We recorded remarkable changes in resistivity in the shallow subsurface at the study area over a period of *one week*.**

These achievements prove two very important points that this study was designed to address: hydrates in the marine environment and near to the extreme of their range, can and do change over time and this change can occur over a period as brief as one week. In the grand scheme of geologic time and oceanographic processes, these are significant finds.

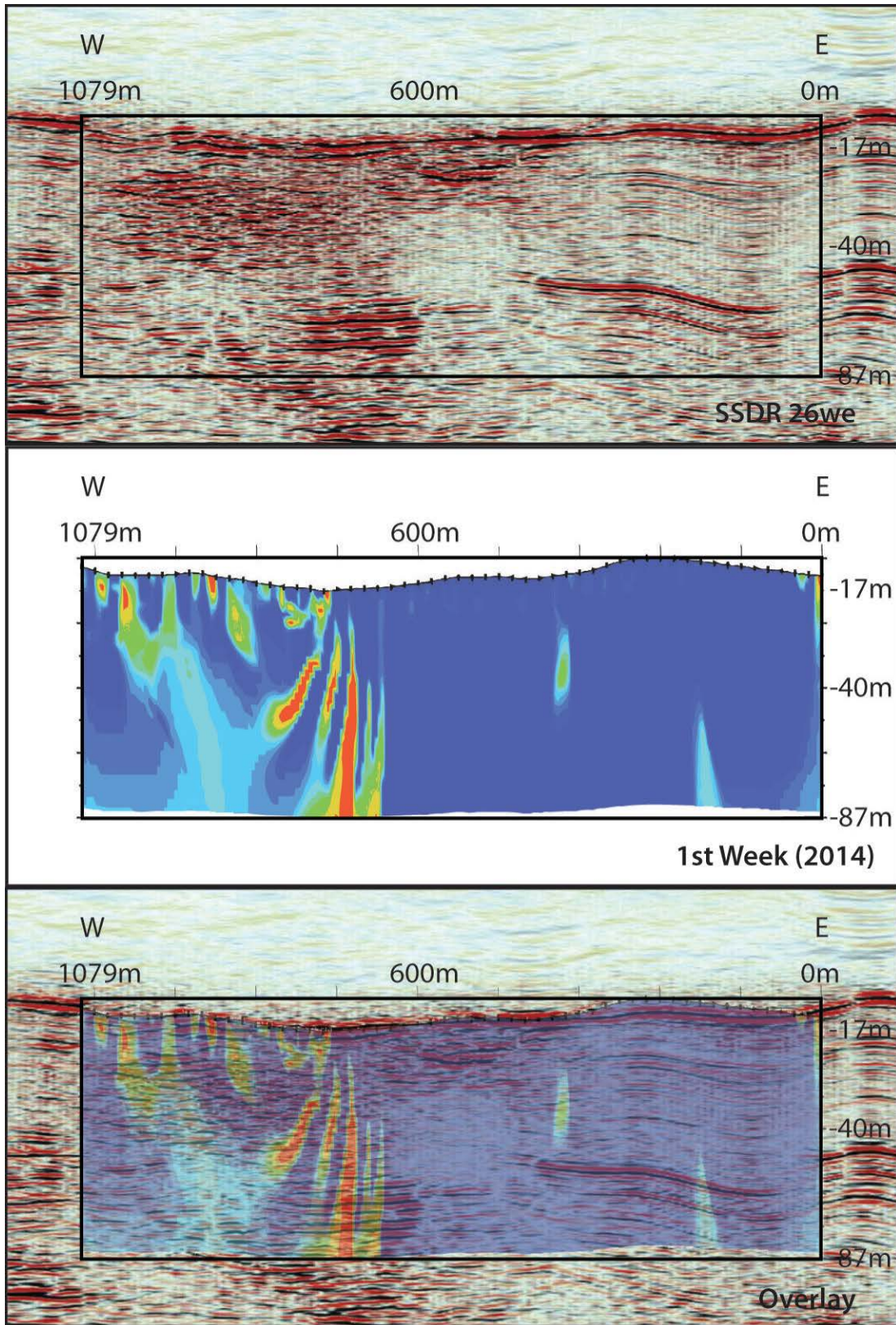


Figure 27. West-to-east SSSR profile, top, and a DCR profile, center, overlain to reveal where resistivity anomalies correspond to structural anomalies.

GRAPHICAL MATERIALS

PAGE

<i>Figure 1. Northern GOM hydrate mound locations. Woolsey Mound is located in MC118 in approximately 900m of water (The top of the HSZ appears in yellow (Milkov&Sassen 2000)).....</i>	<i>12</i>
<i>Figure 2. Seafloor bathymetry at MC118 showing 1) MMS/BOEM research reserve, 2) the carbonate/hydrate Woolsey Mound with crater complexes, sites of the natural venting of hydrocarbons , and 3) large fault to the NE that defines the western boundary of a major slump on the continental slope.....</i>	<i>13</i>
<i>Figure 3. At Woolsey Mound, backscatter (from multibeam) data overlain onto bathymetry highlight both morphologic features and areas of exposed hard-grounds.....</i>	<i>14</i>
<i>Figure 4. SSSR data show features in the shallow sub-seafloor that provide likely targets for gas hydrate accumulation. Together with seafloor bathymetry and backscatter intensity (top left), SSSR presents a picture of what is beneath the mound at MC118. In the SSSR profile, a master fault is shown in yellow. Detail of a pockmark appears in the bottom panel. Note that wipeout zones appear variously in the profile but particularly flanking and within the highlighted features.....</i>	<i>14</i>
<i>Figure 5. Near-bottom observations of Woolsey Mound, MC118. (a) Carbonate blocks on the seafloor. The foreground view is approximately 2m across. (b) Massive slab of hydrate, outcropping on the seafloor. The slab was approximately 1.5m thick and 6m long. (c) and (d) Piston core samples from the upper 15m of the sediment column, showing angular clasts of nearly pure hydrate mixed in mechanically churned, fine-grained sediment.....</i>	<i>15</i>
<i>Figure 6. Schematic diagram of the Gulf of Mexico-Hydrate Research Consortium (GOM-HRC) working model of the methane hydrate distribution at Mississippi Canyon Block 118, circa 2005. Sub-bottom accumulations of gas hydrate were thought to occur, potentially, (1) within the fault zones that serve as the migration paths of thermal gas from depth, (2) within porous strata intersected by the faults, and/or (3) as an irregular layer beneath the overlying carbonate mound.....</i>	<i>16</i>
<i>Figure 7. Shaded topographic relief map of Woolsey Mound, MC118, northern GOM. Bold black lines are resistivity track lines run at MC118 for a 2009 reconnaissance survey.; gray lines indicate the locations of previously collected high-resolution seismic profiles. The red circles mark the locations of high resistivity anomalies. The dashed lines indicate approximate traces of crestal faults previously mapped from depth to the seafloor using a combination of seismic datasets: chirp, SSSR and industry seismic data. Eastings and Northing coordinates are Universal Transverse Mercator (UTM) Zone 16.....</i>	<i>18</i>
<i>Figure 8. Example resistivity line from 2009 reconnaissance survey of MC118. The red arrow marks position of the largest resistivity anomaly observed in the 2009 survey. The location of the anomaly within the MC 118 study area is shown in Figure 7.....</i>	<i>19</i>
<i>Figure 9. The I-Spider™. This custom ROV is equipped with multiple, adjustable cameras and lights, scanning sonar, an altimeter, and USBL locator, all powered within the system. It is used to perform reconnaissance work, to deploy and recover instruments including arrays, and in concert with a working class ROV, can perform rescue missions.....</i>	<i>22</i>
<i>Figure 10. The MMRI/CMRET team designed and built the IPSO lander that houses the computer communications and data storage systems for the DCR array. Instruments and batteries required for the contemporaneous collection of oceanographic data with resistivity data are also mounted on the lander. A 6-month deployment was designed to record changes in the hydrate volume beneath Woolsey Mound and the contemporaneous changes in local physical parameters.....</i>	<i>23</i>
<i>Figure 11. The DCR cable connection to the base of the IPSO lander.....</i>	<i>24</i>
<i>Figure 12. Proposed survey sites for the DCR study include targets and hazards on and around Woolsey Mound.....</i>	<i>25</i>
<i>Figure 13. The DCR cabled array is carefully spooled onto the Pelican’s Dynacon winch and deployed through an extra-wide shiv.....</i>	<i>26</i>
<i>Figure 14. The fiber-optic cable is linked to the I-Spider™ DCR-array-IPSO lander assembly in preparation for deployment.....</i>	<i>26</i>

Figure 15. DCR profiles collected across Woolsey Mound, MC118, April, 2014. Four survey/reconnaissance profiles were collected along the traces shown in black. The IPSO lander and attached DCR array were eventually deployed at the location shown in red. This deployment line lies along a fault from which bubble plumes have been observed at the seafloor and hydrates recovered (via gravity cores) from the shallow subsurface.....28

Figure 16. Initial DCR profiles collected across Woolsey Mound, April, 2014. The positions of the lines within the study area are shown in Figure 15. Vertical dashed lines on profiles 2 and 3 mark intersections of these lines with the fault trace on which Anomaly A occurs, Figure 7. The small anomaly marked “A” is in the same location as Anomaly A shown in Figure 7, corresponding to larger Anomaly A, Figure 8, from the 2009 survey.....29

Figure 17. Dunbar, Stoekel, and Tidwell make final adjustments to the I-Spider™ before sending it on its mission to retrieve the DCR array and instrumented IPSO lander.....30

Figure 18. The grapnel lands and hooks - with two prongs - the east-facing top horizontal bar of the IPSO lander.....30

Figure 19. Recovery of the IPSO lander to the deck of the R/V Pelican was effected using the ship’s crane, hooking the lift-bale once the I-Spider™ had returned the system to the surface.....32

Figure 20. Cutaway diagram of seafloor electrical resistivity electrode. (a) The electrodes on the seafloor resistivity array are hollow cylinders of graphite. Each electrode is connected to one of 56 dedicated conductors, which extends from the electrode to the connector at the instrument end of the array (to the right). Conductors for all other electrodes toward the tail end of the array (left) pass through the center of the electrode. The connection between the copper conductor (green) and the graphite electrode is made by soldering the conductor to a copper pin that is pressed into a hole drilled into the graphite. The connection is then potted to hold the electrode in place and to seal the connection point from any seawater that may have penetrated the jacket of the cable to the left or right of the electrode. (b) Under long deployments at high pressure, seawater penetrates the graphite electrode and envelopes the copper pin, which rapidly corrodes when the electrode is used as a source, leading to a break in the connection to the conductor.....33

Figure 21. Composite of oceanographic data collected during the 4.5 month seafloor deployment from April 14 through September 3, 2014.....35

Figure 22. ADCP components x (east-west), y (north-south), z (vertical), plotted in near-range and in 20m range, together with CTD data, week 1 of deployment.....36

Figure 23. ADCP components x (east-west), y (north-south), z (vertical), plotted in near-range and in 20m range, together with CTD data, week 2 of deployment.....37

Figure 24. ADCP components x (east-west), y (north-south), z (vertical), plotted in near-range and in 20m range, together with CTD data, week 3 of deployment. Note “event” recorded in the conductivity and oxygen saturation values. Possibly “cleansing of the sensor is related to the turbidity event of April 28.....37

Figure 25. DCR Time-lapse profile. The line of section corresponds to Line 5, indicated in Figure 15. (a) Profile collected on April 18, 2014. (b) Profile collected on April 26, 2014. (c) Percent change in resistivities between first and second week. Positive percentage changes correspond to increases in resistivity between the first and second week; Negative percentage changes correspond to decreases in resistivity between the first and second week.....38

Figure 26. ADCP average velocity highlighting near-range net water movement. Turbidity (in white) is plotted over the current velocity.....39

Figure 27. West-to-east SSDR profile, top, and a DCR profile, center, overlain to reveal where resistivity anomalies correspond to structural anomalies.....43

REFERENCES:

- Aharon, P., Roberts, H.H., Snelling, R., (1992), *Submarine venting of brines in the deep Gulf of Mexico: observations and geochemistry*, *Geology* 20, 483–486.
- Barnes, P. M., Lamarche, G., Bialas, J. Henrys, S., Pecher, I., Netzeband, G. L., Greinert, J., Mountjoy, J. J., Pedley, K., and Crutchley, G. (2010), *Tectonic and geological framework for gas hydrates and cold seeps on the Hikurangi subduction margin, New Zealand*, *Marine Geology*, v. 272, p. 26-48.
- Camilli, R., L. Macelloni, V. Asper, M. Woolsey, J. Williams, A. Diercks, C.B. Lutken, K. Sleeper (2009), *Discovery and characterization of cold seeps using a mass spectrometer operating aboard an autonomous underwater vehicle*, AGU fall meeting, San Francisco, CA, December, 17, 2009.
- Chand, S., Mienert, J. Andreassen, K. Knies, J., Plassen, L., and Fotland, B. (2008), *Gas hydrate stability zone modeling in areas of salt tectonics and pockmarks of the Barents Sea suggests and active hydrocarbon venting*, *Marine and Petroleum Geology*, v. 25, p. 625-636.
- Cosenza, P., Ghorbani, A., Camerlynck, C., Rejiba, F., Guérin, R., and Tabbagh, A. (2009), *Effective medium theories for modeling the relationships between electromagnetic properties and hydrological variables in geomaterials: a review*, *Near Surface Geophysics*, 563-578.
- Crutchley, G. J., Pecher, I. A., Gorman, A. R., Henrys, S. A., Greinert, J. (2010), *Seismic imaging of gas conduits beneath seafloor seep sites in a shallow marine gas hydrate province, Hikurangi Margin, New Zealand*, *Marine Geology*, v. 272, p. 114-126.
- Dickens, G. R., Castillo, M. M., and Walker, J. C. G. (1997), *A blast of gas in the latest Paleocene: simulating first-order effects of massive dissociation of oceanic methane hydrate*, *Geology*, v. 25, 259-262.
- Dunbar, J., A. Gunnell, P. Higley, M. Lagmanson (2010), *Seafloor resistivity investigation of methane hydrate distribution in Mississippi Canyon, Block 118, Gulf of Mexico, (expanded abstract)*, Symposium on the Application of Geophysics to Engineering and Environmental Problems, v. 23, p. 835-844.
- Du Frane, W. L., Stern, L. A., Weitemeyer, K. A., Constable, S., Pinkston, J. C., and Roberts, J. J. (2011), *Electrical properties of polycrystalline methane hydrate*, *Geophysical Research Letters*, v. 38, doi:10.1029/2011GL047243.
- Johnson, A. H. (2011), *Global resource potential of gas hydrate – A new calculation*, *Fire in the Ice, Methane Hydrate News Letter*, v. 11, issue 2, p. 1-3.
- Juniper, S. J. (2013), *Monitoring the dynamics of gas hydrate deposits and hydrothermal discharge using the NEPTUNE undersea observatory network*, (abstract) 42nd Underwater Mining Institute, 21-29 October 2013, Rio de Janeiro, Brazil.
- Kennett, J. P. and Fackler-Adams, B. N. (2000), *Relationship of clathrate instability to sediment deformation in the upper Neogene of California*, *Geology*, v. 28, No. 3, p. 215-218.
- Knapp, James H., Camelia C. Knapp, Leonardo Macelloni, Antonello Simonetti, Carol Lutken (2010), *Subsurface Structure and Stratigraphy of a Transient, Fault-Controlled Thermogenic Hydrate System at MC-118, Gulf of Mexico*, AAPG 2010 Annual Convention Oral Presentation, Abstracts Volume, p.134.
- Kvenolden, K. A. (2002), *Methane hydrate in the global organic carbon cycle*, *Terra Nova*, v. 14, p. 302-306.
- Lapham, L., J. Chanton, C. Martens, K. Sleeper and J. Robert Woolsey (2008), *Microbial activity in surficial sediments overlying acoustic wipeout zones at a Gulf of Mexico cold seep*, *Geochemistry, Geophysics, Geosystems*, Volume 9, No. 6, June 4.
- Liu, X., and Fleming, P.B. (2007), *Dynamic multiphase flow model of hydrate format marine sediments*. *J. Geophys. Res.*; 112 (B03101): 1-23.
- Liu, X. and Flemings, P. (2009), *Dynamic response of oceanic hydrates to sea level drop*, *Geophysical Research Letters*, v. 36, L17308, doi:10.1029/2009GL039821.
- Loncke, L. and Mascle, J. (2004), *Mud volcanoes, gas chimneys, pockmarks, and mounds in the Nile, deep-sea fan (Eastern Mediterranean): geophysical evidences*, *Marine and Petroleum Geology*, v. 21, p. 669-689.
- MacDonald, Ian R., William W. Sager, Michael B. Peccini (2003), *Gas hydrate and chemosynthetic biota in mounded bathymetry at mid-slope hydrocarbon seeps: Northern Gulf of Mexico*, *Marine Geology* 198 (2003) 133-158.
- MacDonald, I. R., Bender, L.C., Vardaro, M., Benard, B., and Brooks, J. (2005), *Thermal and visual time-series at a seafloor gas hydrate deposit on the Gulf of Mexico Slope*, *Earth and Planetary Science Letters*, v. 233, p. 45-59.

- Macelloni, Leonardo, Bradley M Battista, Camelia C Knapp (2011), *Optimal Filtering High-Resolution Seismic Reflection Data Using a Weighted-Mode Empirical Mode Decomposition Operator*. Journal of Applied Geophysics, 75 (2011) 603-614.
- Macelloni, Leonardo, Antonello Simonetti, James H Knapp, Camelia C Knapp, Carol B Lutken (2012), *Multiple resolution seismic imaging of a shallow hydrocarbon plumbing system, Woolsey Mound, Northern Gulf of Mexico Gulf of Mexico*. Marine and Petroleum Geology 38:128-142.
- Macelloni, Leonardo, Charlotte Brunner, Simona Caruso, Carol Lutken, Marco D'Emidio, Laura Lapham (2013), *Spatial distribution of seafloor biogeological and geochemical processes as proxies of fluid flux regime and evolution of a carbonate/hydrates mound, northern Gulf of Mexico*, Deep-Sea Research I 74 (2013) 25–38.
- Macelloni, L., C.B. Lutken, S. Garg, A. Simonetti, M. D'Emidio, R.M. Wilson, K. Sleeper, L.L. Lapham, T. Lewis, M. Pizzi, J.H. Knapp, C.C. Knapp, J. Brooks, T.M. McGee (2015), *Heat-flow regimes and the hydrate stability zone of a transient, thermogenic, fault-controlled hydrate system (Woolsey Mound, northern Gulf of Mexico)*, Marine and Petroleum Geology, 59: 491-504.
- Milkov, A. V. (2000), *Worldwide distribution of submarine mud volcanoes and associated gas hydrates*, Marine Geology, v. 167, p. 29-42.
- Milkov, A.V. and R. Sassen (2000), *Thickness of the gas hydrate stability zone, Gulf of Mexico continental slope*, Marine and Petroleum Geology, v. 17, pp. 981-991.
- Milkov, A.V., Sassen, R. (2001), *Estimate of gas hydrate resource, northwestern Gulf of Mexico continental slope*. Marine Geology 179, 71 – 83.
- Netzeband, G. L., Krabbenhoeft, A., Zillmer, M., Petersen, C. J., Papenberg, C., and Bialas, J. (2010), *The structures beneath submarine methane seeps: seismic evidence from Opouawe Bank, Hikurangi Margin*, Marine Geology, v. 292, p. 59-70.
- Reagan, M.T. and Moridis, G.J. (2007), *Oceanic Gas hydrate instability and dissociation under climate change scenarios*, Geophysical Research Letters, v. 34, L22709, doi: 10.1029/2007GL031671.
- Riedel, M., Willoughby, E. C., & Chopra, S. (Eds.). (2010). Geophysical characterization of gas hydrates (Vol. 14). Society of Exploration Geophysicists.
- Roberts, H. H., & Aharon, P. (1994). Hydrocarbon-derived carbonate buildups of the northern Gulf of Mexico continental slope: a review of submersible investigations. Geo-Marine Letters, 14(2-3), 135-148.
- Sheets, R. A. (2002), *Use of Electrical Resistivity to Detect Underground Mine voids in Ohio*, U.S. Geological Survey, Water-Resources Investigations Report 02-4041, Reston, VA, 10 p.
- Sheets, R. A. (2002), *Use of Electrical Resistivity to Detect Underground Mine voids in Ohio*, U.S. Geological Survey, Water-Resources Investigations Report 02-4041, Reston, VA, 10 p.
- Simonetti, Antonello, James H. Knapp, Camelia C. Knapp, Leonardo Macelloni, Carol B. Lutken (2011), *Defining the hydrocarbon leakage zone and the possible accumulation model for marine gas hydrates in a salt tectonic driven cold seep: examples from Woolsey Mound, MC118, northern Gulf of Mexico*, Proceedings of the 7th International Conference on Gas Hydrates (ICGH 2011), Edinburgh, Scotland, United Kingdom, July 17-21.
- Simonetti, Antonello, James H. Knapp, Kenneth Sleeper, Carol B. Lutken, Leonardo Macelloni, Camelia C. Knapp (2013), *Spatial Distribution of Gas Hydrates from High-Resolution Seismic and Core Data, Woolsey Mound, Northern Gulf of Mexico*, Marine and Petroleum Geology 44 (2013) 21-33.
- Sleeper, K., Lowrie, A., Bosman, A., Macelloni, L. and Swann, C.T., 2006, *Bathymetric mapping and high resolution seismic profiling by AUV in MC 118 (Gulf of Mexico)*. Offshore Technology Conference. OTC-18133.
- Sleeper, K. and Lutken, C. (2008), *Activities Report for Cruise GOM1-08-MC118 aboard the R/V Pelican Sampling and Deployment Cruise Mississippi Canyon Federal Lease Block 118, Northern Gulf of Mexico*, Center For Marine Resources And Environmental Technology and Seabed Technology Research Center, University Of Mississippi, April 22-28, 2008, 18pp.
- Torres, M., Trehu, A., Riedel, M., Paull, C., Davis, E. (2007) Report of the Gas-Hydrate Observatories Workshop (GHOB) Portland Oregon, July 18-20, 2007.
- Xu, W. and Lowell, R. P. (2001), *Effect of seafloor temperature and pressure variations on methane flux from a gas hydrate layer: Comparison between current and late Paleocene climate conditions*, Journal of Geophysical Research, v. 106, no. B11, p. 26,413-26,423.
- Wagner, F. M., Moller, M., Schmidt-Hattenberger, C. Kempka, T., and Maurer, H. (2013), *Monitoring freshwater salinization in analog transport models by time-lapse electrical resistivity tomography*, Journal of Applied Geophysics, v. 89, p. 84-95.

ACRONYMS AND ABBREVIATIONS

2D	2-dimensional
3D	3-dimensional
ADCP	Acoustic Doppler Current Profiler
AUV	Autonomous underwater vehicle
BHSZ	Base of hydrate stability zone
BOEM	Bureau of Ocean Energy Management
bsf	below seafloor
CMRET	Center for Marine Resources and Environmental Technology
CRP	Continuous Resistivity Profiling
CSEM	controlled source electromagnetic
CTD	instrument that measures and records conductivity (salinity), temperature, and pressure (depth)
DC	Direct Current
DCR	Direct Current Resistivity
DOE	Department of Energy
EM	electromagnetic
GOM	Gulf of Mexico
GOM-HRC	Gulf of Mexico Hydrates Research Consortium
GRT	geoelectrical resistivity tomography
HSZ	Hydrate Stability Zone
IDP	Integrated Data Processing unit
IPSO	Integrated Portable Seafloor Observatory
I-Spider™	Integrated Scientific Platform for Instrument Deployment and Emergency Recovery
kg	kilograms
LUMCON	Louisiana Universities Marine CONSortium
m	meters
mbsf	meters below seafloor
MC118	Mississippi Canyon, Federal lease Block 118, northern Gulf of Mexico
MMRI	Mississippi Mineral Resources Institute
MMS	Minerals Management Services
MS/SFO	Monitoring Station/Seafloor Observatory
NIUST	National Institute for Undersea Science and Technology
Ohm-m	Ohm-meters
pc	personal computer
ppm	parts per million
ppt	parts per thousand
ROV	Remotely operated vehicle
R/V	Research Vessel
SDI	Specialty Devices, Inc.
SSD	Station Service Device
SSDR	Shallow-Source-Deep-receiver
STP	standard temperature and pressure
TrakLink	navigation software
UM	University of Mississippi
USBL	Ultra-Short Baseline
UTM	Universal Transverse Mercator

APPENDIX A: Data Inventory:

1. **multibeam** (*Okeanos Explorer*); hull-mounted system ~25m resolution; 2011; available online.
2. **multibeam** of the entire block at 40m above seafloor, 200m spacing; ~1.5m resolution.; acquired in May, 2005, by C&C Technologies; reprocessed most recently in 2011 at MMRI; CMRET owns it.
3. **multibeam** full Eagle Ray (AUV) survey at 50m above seafloor, 200m line spacing; ~1.5m resolution; Sept-Oct, 2012; only extraneous data removed; belongs to NIUST.
4. **multibeam** full ER survey of Woolsey Mound at 15m above seafloor, 60m line spacing (.5m resolution); Sept-Oct, 2012; only extraneous data removed; belongs to NIUST.
5. **chirp** of the entire block at 40m from seafloor, 200m spacing; 10cm resolution; May, 2005, by C&C Technologies; CMRET owns it.
6. **ppchirp** full ER survey at 50m above seafloor and 200m line spacing; 10cm resolution; Sept-Oct, 2012; not post-processed; belongs to NIUST.
7. **ppchirp** full ER survey of Woolsey Mound at 15m above seafloor, 60m line spacing; 10cm resolution; Sept-Oct, 2012; not post-processed; belongs to NIUST.
8. **gravity cores**; <10m in length; January, 2005; May, 2005; October, 2005; April, 2008; electric logs on representative samples, all logged and described by hand; all logs owned by CMRET.
9. **Jumbo Piston Cores** (5); 15-18m in length; January 2011; all logged and described by hand. Some electric logs run at Stennis; all logs belong to CMRET.
10. **push-cores** recovered by the SSD; <.5m; June, 2007; November, 2007; September, 2010; some processed for microbial populations; sent to various Consortium members, i.e. not onsite.
11. **seismic data** from MC118 (high resolution Surface-source-deep-receiver, SDR), 2006.
12. **video and photodata** that have been made available to us for a variety of purposes.
13. full **Mola Mola photosurvey** of key portions of Woolsey Mound; 3m off the seafloor; Sept-Oct, 2012; being mosaicked at NIUST; belongs to NIUST.
14. **side-scan** from Woolsey Mound; Navy surveys using new AUV: April, 2011.
15. **side-scan** from about ½ of Woolsey Mound; NR-1; 2007.